PhD Thesis

On-chip multiplex PCR identification of automatically retrieved single microchimeric cells

Single cell DNA fingerprint analysis as a gold standard of sex-independent confirmation of fetal identity of cells present in the circulation of pregnant women and as a target for non-invasive genetic diagnosis

Submitted in total fulfillment of the requirements of the degree of

Doctor of Medical Sciences (Dr.scient.med.)

performed at the
Center of Molecular Medicine,
Institute for Cell Biology, Histology and Embryology, Medical University of Graz

Dipl.-Ing. Thomas Kroneis
matriculation number: 9211411

PhD Committee:
Assoc Univ.-Prof. Dr. med. Peter Sedlmayr (supervisor)
Assoc. Univ.-Prof. Mag. Dr. scient. med. Dr. rer. nat. Erwin Petek (co-supervisor)
Univ.-Prof. Dr. med. Gottfried Dohr

June 3, 2009 Dipl.-Ing. Thomas Kroneis

Preamble

Eidesstattliche Erklärung

Ich erkläre ehrenwörtlich, dass ich die vorliegende Arbeit selbständig und ohne fremde Hilfe verfasst, andere als die angegebenen Quellen nicht verwendet und die den benutzten Quellen wörtlich oder inhaltlich entnommenen Stellen als solche kenntlich gemacht habe. Die Arbeit an der Dissertation und daraus entstandener Publikationen wurde gemäß den Regeln der „Good Scientific Practice“ durchgeführt.

Declaration

This is to certify that this thesis comprises only my original work towards the PhD except where indicated. Due acknowledgement has been made in the text to all other material used. Throughout this thesis and all related publications I observed “Good Scientific Practice”.

June 3, 2009 Dipl.-Ing. Thomas Kroneis

Dedicated to most wonderful Kathrin
and my beloved children Maria, Max, and Leonhard

Publications

During the course of this project, a number of public presentations have been made which are based on the work presented in this thesis. They are listed here for reference.

2009

Journal Articles

Kroneis, T; Gutstein-Abo, L; Kofler, K; Hartmann, M; Hartmann, P; Alunni-Fabbroni, M; Walcher, W; Dohr, G; Petek, E; Guetta, E; Sedlmayr, P, 2009 Automatic retrieval of single microchimeric cells and verification of identity by on-chip multiplex PCR.
J Cell Mol Med. 2009 May 19. [Epub ahead of print]

Unpublished conference presentations

Kroneis, T; Sedlmayr, P, 2009. Low-volume PCR in single cell analysis. Carl Zeiss Microdissection Workshop "Praktische Anwendung der non-contact laser capture microdissection (LCM) Technik am PALM MicroBeam System"; Mar 19-20, 2009; Munich, GERMANY. 2009. -Oral Communication

2008

Conference papers, proceedings, abstracts

Kroneis, T; Geigl, JB; Waldispühl-Geigl, J; Alunni-Fabbroni, M; Petek, E; Walcher, W; Dohr, G; Sedlmayr, P, 2008 Contamination-free Analysis of Single Cells in Cell-based Non-invasive Prenatal Diagnosis. European Journal of Human Genetics, suppl. 2 2008; 16: The European Human Genetics Conference 2008; May 31-3, 2008; Barcelona, SPAIN. Oral Communication

Kroneis, T; Alunni-Fabbroni, M; Johannes, T; Kofler, K; Walcher, W; Dohr, G; Petek, E; Sedlmayr, P, 2008 Merging of Sample Processing, Semi-automated Detection, and Molecular Genetic Analysis for Process-like Single-cell Analysis. Abstractband des Workshops 2008; Safe PHD Student Workshop/Non Invasive Prenatal Diagnosis; Feb 24-25, 2008; Bologna, ITALY. Oral Communication

Unpublished conference presentations

Kroneis, T; Geigl, JB; Alunni-Fabbroni, M; Hartmann, P; Johannes, T; Guetta, E; Abo-Gutstein, L; Coata, G; Petek, E; Sedlmayr, P, 2008 Low-volume on-chip single cell analysis using whole genome amplification and DNA fingerprinting in non-invasive prenatal diagnosis and beyond. SAFE Final PhD Student Workshop; Oct 25, 2008; Vienna, AUSTRIA. 2008. Oral Communication

Kroneis, T; Alunni-Fabbroni, M; Petek, E; Dohr, G; Sedlmayr, P, 2008 Nicht-invasive Pränataldiagnostik auf Basis einzelner Zellen. 24. Jahrestagung der Österreichischen Gesellschaft für Reproduktionsmedizin und Endokrinologie; Oct 9-11, 2008; Graz, AUSTRIA. 2008. Oral Communication

Kroneis, T; Johannes T, Alunni-Fabbroni, M; Kofler, K; Petek, E; Dohr, G; Sedlmayr P, 2008. DNA fingerprinting analysis of single cells via automated detection, laser microdissection, and low-volume on-slide PCR. Life Sciences 2008; Sep 22-24, 2008; Graz, AUSTRIA. 2008.-Poster

Kroneis, T; Geigl, JB; Waldispühl-Geigl, J; Alunni-Fabbroni, M; Petek, E; Dohr, G; Sedlmayr P, 2008 Towards contamination-free rare cell diagnosis. SAFE Final General Assembly Meeting; May 29-30, 2008; Tarragona, SPAIN. 2008. Oral Communication

Kroneis, T, 2008. Techniques in Single Cell Analysis. PALM-Workshop; The Key to purity: Microdissection with a Laser; Mar 10, 2008; Zurich, SWITZERLAND. 2008. Oral Communication

2007

Unpublished conference presentations

Kroneis, T; Geigl, JB; Kofler, K; Petek, E; Walcher, W; Dohr, G; Sedlmayr P, 2007 Nicht-invasive Pränataldiagnostik auf Basis fötaler Zellen. 8. Tagung: Zellbiologie, Histologie und Embryologie; Oct 5-6, 2007; Graz, AUSTRIA. 2007. Oral Communication

Kroneis, T, 2007. AmpliGrid in der nicht-invasiven Pränataldiagnose. Oct 2, 2007; Graz, AUSTRIA. 2007. Oral Communication

Sedlmayr, P; Kroneis, T; Kofler, K, 2007. Towards economically feasible cell-based non-invasive prenatal diagnosis. Workshop on Non-invasive Prenatal Diagnosis. 2nd Yazd International Student Award and Congress in Reproductive Medicine; May 10, 2007; Yazd, Iran. 2007. Oral Communication

Kroneis, T; Kofler, K; Havlicek, T; Schmied, R; Sedlmayr, P, 2007. Evaluation of slide-based cytometry by use of Metafer Systems for non-invasive prenatal diagnosis SAFE, 3rd Annual General Assembly; Jan 29-31, 2007; Bristol, GREAT BRITAIN. 2007. Oral Communication

Kroneis, T; Kofler, K; Havlicek, T; Schmied, R; Sedlmayr, P, 2007. Single fetal cell based approach in non-invasive prenatal diagnosis. SAFE, 3rd Annual General Assembly; Jan 29-31, 2007; Bristol, GREAT BRITAIN. 2007. Oral Communication

Kofler, K; Kroneis, T; Geigl, JB; Havlicek, T; Schröder, J; Speicher, M; Sedlmayr, P, 2007. New Trophoblast Specific Antibodies – The Search For Fetal Cells Goes On. SAFE, 3rd Annual General Assembly; Jan 29-31, 2007; Bristol, GREAT BRITAIN. 2007. Poster

2006

Conference papers, proceedings, abstracts

Kroneis, T; Kofler, K; Havlicek, T; Schmied, R; Johannes, T; Petek, E; Sedlmayr, P, 2006. Single fetal cell based approach in non-invasive prenatal diagnostics Am. J. Reprod. Immunol. 56(1):47-48. 4th European Congress of Reproductive Immunology; Jul 5 – 9; Graz. Poster

Unpublished conference presentations

Kroneis, T, 2006. From Man to Machine: Application of a Cell Detection Software on Fetal Cells. Special Non-Invasive Advances in Fetal and Neonatal Evaluation Network; Oct 19, 2006; Bernried, GERMANY. 2006. Oral Communication

Kroneis, T; Kofler, K; Havlicek, T; Schmied, R; Johannes, T; Sedlmayr, P, 2006. Slide-based Cytometry and Laser Microdissection in Non-Invasive Prenatal Diagnosis. 4th European Congress of Reproductive Immunology; Jul 5, 2006; Graz, AUSTRIA. 2006. Poster

Acknowledgements

I would like to express my deepest appreciation to my supervisor Peter Sedlmayr. Throughout the years he has been routing my scientific course giving just minor corrections now and then being a shrewd mind. This freedom was both confusing and liberating but in the end necessary to acquire scientific skills being a credit to PhD.

I am indebted to my co-supervisor Erwin Petek for introducing me to human genetic analysis and its pitfalls. His remarks caused some crucial ideas coming to my mind that increased the impact of my work culminating in a nice paper.

Many ideas would not have been thought and much of the work would not have been done in the recent years if there had not been two members of the institute, namely Trude Havlicek and Rudi Schmied. Being a congenial lab coworker, Trude and I perfectly complemented each other. The hours Rudi and I spent on optimizing cell detection, microdissection, microscope settings and on inventing are among the most precious. Thanks again for your high engagement and your commitment.

A special thank goes to all my fellow PhD students Chrisi, Gerit, Kiki, Kristina, Regine-Susanne and Sonja providing a stimulating and fun environment in which to learn and grow (and eat).

I would like to thank all my SAFE PhD and MD fellows for having a great time at the PhD student meetings and workshops during the time we have been members of a great network of excellence. My special thanks go to Francesco Crea, Gerasimos Dimisianos, Liat Gutstein-Abo, Thomas Hahn, Prasad Koller, Debbie Maddocks, Tracey Madgett, Toni McCollum, Sina Müller, and Wei Yuan

I am grateful to the SAFE Network of Excellence (LSHB-CT-2004-503243) for granting me a PhD studentship. I enjoyed being a part of this network as it was both a personal and scientific gain.

Most importantly I wish to thank my parents Christl and Herbert Kroneis for their loving, long standing and familiar support. Without your help I might have lost track.

Without the loving and understanding care of Kathrin, tough Maria, brave Max and lively Leonhard this work would not have been written. I love you.

Zusammenfassung

Die Analyse seltener Zellen ist ein komplexes Unterfangen. Das gilt vor allem für die Analyse fötaler Zellen in der nicht-invasiven Pränataldiagnostik, da sie nur in geringer Anzahl im peripheren Blut von Schwangeren zirkulieren. Die Analyse von so genannten seltenen Zellen, zu denen auch die zirkulierenden fötalen Zellen zählen, stellt hohe Anforderungen an die Analysentechnik, da eine Kontamination durch maternale Zellen unbedingt ausgeschlossen werden muß. Unter den vorliegenden Bedingungen der Analyse seltener Zellen vergehen allerdings Methoden basierend auf der Verwendung selbst hochspezifischer Biomarker. In der vorliegenden Arbeit habe ich eine Methode zur genetischen Identifikation seltener Zellen entwickelt. Dabei werden vorangereicherte Zellen mittels Immunfluoreszenz gefärbt und positive Zellen mit Hilfe eines Scan Systems automatisch detektiert. Die detektierten Kandidatenzellen werden einzeln mikrodissektiert und deren DNA Profil auf Chip Technologie im Mikroliter-Maßstab mittels 16plex-PCR ermittelt. Die Aussagekraft der Methode wurde mithilfe von Proben erstellt, die entweder eine Mischung aus Zellen nicht-verwandter oder verwandter Individuen enthielten. DNA Profile konnten in 74% (55/74) aller getesteten Einzelzellen erstellt werden. Die PCR-Effizienz heterozygoter Genloci lag bei 59,2% (860/1452). Die Identifikation von Zellen mittels DNA Profil wurde von Zellen angereichert aus Blut und isoliert aus Geweben durchgeführt. Alle Zellen analysiert aus Zellsuspensionen nicht-verwandter Zellen konnten eindeutig identifiziert werden (12/12). Im Fall verwandter Zellen, die im halben Chromosomensatz übereinstimmen, konnten 37 von 43 (86%) Einzelzellen eindeutig über ihr DNA-Profil identifiziert werden. Die Ergebnisse zeigen, daß die Erstellung von DNA-Profilen einzelner Zellen möglich ist und hohes Identifikationspotential besitzt. Aus diesem Grund empfehle ich die Erstellung von DNA Profilen zur standardisierten Identifikation seltener Zellen auf der Basis einzelner Zellen

Schlagwörter: Pränataldiagnostik, Analyse seltener Zellen, Mikrochimerismus, Einzelzell-PCR

Abstract

The analysis of rare cells is a complex task. This is especially true when cells representing a fetal microchimerism are to be utilized for the purpose of non-invasive prenatal diagnosis since it is both imperative and difficult to avoid contaminating the minority of fetal cells with maternal ones. Under these conditions, even highly specific biochemical markers are not perfectly reliable. Thus, I developed a method to verify the genomic identity of rare cells that combines automatic screening for enriched target cells (based on immunofluorescence labeling) with isolation of single candidate microchimeric cells (by laser microdissection and subsequent laser-catapulting) and low-volume on-chip multiplex PCR for DNA fingerprint analysis. The power of the method was tested by using samples containing mixed cells of related and non-related individuals. Single cell DNA fingerprinting was successful in 74% (55/74) of the cells analyzed with a PCR efficiency of 59.2% (860/1452) for heterozygous loci. The identification of cells by means of DNA profiling was performed on both cells enriched from blood and cells isolated from tissue. Identification was achieved in 100% (12/12) of non-related cells in artificial mixtures and in 86% (37/43) of cells sharing a haploid set of chromosomes. Thus, I suggest DNA profiling as a standard for the identification of microchimerism on a single cell basis.

Key words: microchimerism, prenatal diagnosis, rare cell analysis, single cell PCR

Table of Contents

Publications iv
Acknowledgements vii
Zusammenfassung viii
Abstract ix
Table of Contents x
Abbreviations xiii
Figures xvii
Tables xvii
1 Introduction 1
1.1 Prenatal diagnosis 1
1.2 Non-invasive prenatal diagnosis (NIPD) 1
1.2.1 Cell-free fetal DNA and RNA 1
1.2.2 Circulating fetal cells 2
1.3 Minimally invasive prenatal diagnosis 9
1.4 Automated scanning 10
2 Aim 13
3 Materials 14
4 Methods 17
4.1 Ethics 17
4.2 Basic protocols 17
4.3 Antibodies used for enrichment and staining purposes 17
4.4 Cell sampling from cord blood 19
4.5 Cell sampling from chorionic villous and decidual tissues 20
4.5.1 Mechanical digestion 20
4.5.2 Enzymatic digestion 20
4.6 Artificial mixtures of JAR choriocarcinoma cells and peripheral blood mononuclear cells (PBMNCs) 21
4.7 Automated rare cell detection 22
4.7.1 Training RCDetect software 22
4.7.2 Rare cell detection 23
4.8 Laser microdissection and pressure catapulting (LMPC) 23
4.9 Low-volume on-chip cell lysis and multiplex PCR 24

4.9.1 Cell lysis 24
4.9.2 Multiplex-PCR 25
4.10 Purification of PCR fragments 26
4.11 Fragment analysis 26
4.12 PCR efficiency and DNA profiles 26
5 Results 28
5.1 Development of a classifier for multi cell type detection 28
5.1.1 Basic classifier 28
5.1.2 Classifier optimization 29
5.1.3 Using an optimized classifier proved automatic cell detection to be superior to individual screening 31
5.1.4 Detection of a Hbγ^+ cell enriched from peripheral blood of a pregnant woman (12th week of gestation) 32
5.1.5 Settings of classifier “Test Obj 10x” 33
5.2 Development of cell capture setting on AmpliGrid slides 35
5.3 Performance of rare cell analysis 35
5.3.1 PCR efficiency – a parameter for process-related DNA degradation 36
5.3.2 Genetic fingerprinting – distinguishing between cells originating from different individuals 39
6 Discussion 47
6.1 Automated detection 47
6.2 Performance of rare cell analysis 48
6.2.1 Fixation, labeling, scanning and laser microdissection is compatible with single cell DNA fingerprinting 48
6.2.2 Single cell DNA-profiles enable to distinguish between cells sharing a haploid set of chromosomes 51
7 Appendix – Basic Protocols 53
7.1 Basic enrichment protocols 53
7.1.1 Buffers and solutions 53
7.1.2 Density gradient centrifugation 54
7.1.3 Density gradient centrifugation using non-physiological conditions 54
7.1.4 Magnetic cell separation protocol 55
7.2 Basic cytocentrifugation protocol 55

7.3 Fixation and labeling 56
7.3.1 Histochemistry 56
7.3.2 Direct immunofluorescence labeling 56
7.3.3 Indirect immunofluorescence labeling 57
Literature 58

Abbreviations

#	number
°C	degrees Celsius
µg	microgram(s)
µl	microliter
µm	micrometer
µM	micromolar
1°	first
2°	second
2plex	duplex
45,X0	monosomy X, Turner Syndrome
47,+21	trisomy 21, Down Syndrome
47,XXX	Triple X Syndrome
47,XXY	Klinefelter Syndrome
47,XY,+13	trisomy 13, Patau Syndrome (male)
47,XY,+18	trisomy 18, Edwards Syndrome (male)
47,XYY	XYY trisomy
69, XXX	triploidy
A	Adenine
a. dest.	aqua destillata
AC	amniocentesis
ACD-A	Anticoagulant Citrate Dextrose Solution A
ADI	allele drop-in
ADO	allele drop out
approx.	approximately
bp	base pairs
BSA	bovine serum albumin
C	Cytosine
CD	cluster of differentiation
cffDNA	cell-free fetal DNA
CGH	chromosomal genomic hybridization
CStain	counter stain
CVS	chorionic villous sampling

d	double
ddH_2O	double distilled water
DAPI	4',6-diamidino-2-phenylindole
dl	deciliter
DNA	deoxyribonucleic acid
ε	epsilon
EDTA	ethylenediaminetetraacetic acid
$F(ab')_2$	antigen binding fragments linked by disulfide bonds
FACS	fluorescence activated cell sorting
FBS	fetal bovine serum
FISH	fluorescence*in situ* hybridization
FITC	fluorescein isothiocyanate
$FITC^-$	FITC-negative
$FITC^+$	FITC-positive
γ	gamma
g	gram(s)
G	Guanine
GABRB3	Gamma-aminobutyric acid (GABA) A receptor, beta 3
GPA	glycophorin A
$GZ158^+$	GZ158-positive
$(GZ158/GZ112)^+$	GZ158/GZ112 positive
h	hour(s)
hAB	human AB
Hbγ	fetal hemoglobin (gamma chain)
Hbε	embryonic hemoglobin (epsilon chain)
Hbζ	embryonic hemoglobin (zeta chain)
$Hb\gamma^+$	Hbγ-positive
$Hb\varepsilon^+$	Hbε-positive
$Hb\zeta^+$	Hbζ-positive
HBSS	Hank's Buffered Salt Solution
HLA-G	human leukocyte antigen G
$HLA\text{-}G^+$	HLA-G positive

HRP	horse radish peroxidase
HT-29	human adenocarcinoma cell line (Caucasian, colon, grade II)
IF	immunofluorescence, immunofluorescently
IgG1	Immunoglobulin G subclass 1
ILS 600	internal lane standard 600
IR	interruption
ISET	isolation by size of epithelial tumor cells
$I_{t,max}$	Maximum Integration Time
IUL	intrauterine lavage
kb	kilobases
LMPC	Laser Microdissection and Pressure Catapulting
M	molar
MACS	magnetic cell sorting
mg	milligram(s)
min	minute(s)
ml	milliliter
mM	millimolar
mm	millimeter
mm^2	square millimeter(s)
MNC(s)	mononuclear cell(s)
mOsm	milliosmolal
mRNA	messenger RNA
n	number
NaCl	natrium chloride
NIPD	non-invasive prenatal diagnosis
nm	nanometer
NRBC(s)	nucleated red blood cell(s)
O/N	over night
PBMNC(s)	peripheral blood mononuclear cell(s)
PBS	phosphate buffered saline
PCR	polymerase chain reaction
PEN	polyethylene naphthalate
PEP	primer extension preamplification

pg	picogram(s)
pH	negative decimal logarithm of the hydrogen ion activity
PRINS	primed *in situ* labeling
pts	points
QF-PCR	quantitative fluorescent PCR
RhD	Rhesus factor gene loci
RhD	Rhesus factor (RhD antigen)
RNA	ribonucleic acid
rpm	revolutions per minute (radial-dependent centrifugation unit)
s	second(s)
SK-MEL-30	Human melanoma cell line (Caucasian)
SNP(s)	single nucleotide polymorphism(s)
STR	short tandem repeats
T	Thymine
TCC	transcervical cell samples
TO-PRO-3$^-$	TO-PRO-3-negative
TO-PRO-3$^+$	TO-PRO-3-positive
vs.	versus
w/o	without
WGA	whole genome amplification
X	X chromosome
xg	fold gravity (centrifugation unit)
Y	Y chromosome
Y$^+$	Y chromosome-positive
yrs	years
ζ	zeta

Figures

Figure 1: GZ158 staining pattern on 1° trimester placenta and decidua 18
Figure 2: FACS analysis of 1° trimester trophoblast cell fraction 19
Figure 3: Scan field image used for classifier development 28
Figure 4: Setting of basic classifier „18-07-05 z200” 29
Figure 5: Detection of different cell types 30
Figure 6: Scanning performance: 10x objective versus 20x objective 31
Figure 7: Hbγ^{+} erythroblast detected at 12 weeks of gestation 33
Figure 8: Parameter settings of “Test Obj 10x” classifier 34
Figure 9: Focus parameter settings of “TK10 small grid” 34
Figure 10: PEN membrane slide - chip assembly 35

Tables

Table 1: Consumables 14
Table 2: Antibodies 14
Table 3: Reagents, solutions, buffers and media 15
Table 4: Kits 15
Table 5: Tissues and cell lines 16
Table 6: Software 16
Table 7: Equipment 16
Table 8: Density gradient used for erythroblast or trophoblast cell enrichment 21
Table 9: Laser Microdissection and Pressure Catapulting settings 24
Table 10: Cell lysis and PCR mixes (for 30 reactions) 25
Table 11: PowerPlex 16 System amplification protocol (ASC400D SlideCycler) 25
Table 12: Detection efficiency outcome: RCDetect vs. individual scanning 32
Table 13: DNA profiles of sample types 36
Table 14: PCR performance in pooled and single cell samples from two different experimental settings 38
Table 15: PCR efficiency based on the number of cells used as template 38
Table 16: DNA profiles of JAR cells and PBMNC sample #2 40
Table 17: DNA profiles of JAR cells and PBMNC sample #3 41
Table 18: DNA profiles of fetal and maternal cells obtained from tissue from termination of pregnancy (IR #1) 42

Table 19: DNA profiles of fetal and maternal cells obtained from interruption material (IR #3) 43
Table 20: 10x stock solutions of PBS (100mM) 53
Table 21: PBS/EDTA 53
Table 22: 10x stock solution of MACS buffer 53
Table 23: Anticoagulant Citrate Dextrose Solution A (ACD-A) 53

1 Introduction

1.1 Prenatal diagnosis

Current procedures in prenatal diagnostics such as chorionic villous sampling (CVS) and amniocentesis (AC) increase the risk of fetal loss. After CVS, performed between the 10th and 12th week of pregnancy, and early AC, performed between the 11th and 13th week of pregnancy, this risk of fetal loss was published to be 4.8% and 5.3%, respectively (1). According to a study by Hoesli *et al.*, spontaneous fetal loss occurred in 3.86% (maternal ages at 16-19 yrs: 2.94%; 20-24 yrs: 3.2%; 25-29 yrs: 3.39%; 30-34 yrs: 3.89%; 35-39 yrs: 7.82; 40-45 yrs: 50%; >45 yrs: 50%) of surveyed pregnancies (2) indicating that CVS and early AC increase the risk of fetal loss by at least 1%. A review summarizing 29 studies of a total of 68,119 mid-trimester AC reported the fetal loss rate to be 1.68% compared to 1.08% in the control group (3). Thus, mid-trimester amniocentesis accounts for an increase of fetal loss by 0.6%.

1.2 Non-invasive prenatal diagnosis (NIPD)

In the recent years methods were developed allowing to non-invasively obtaining fetal DNA and RNA for molecular genetic analysis. The two main approaches use either circulating fetal cells or cell-free fetal nucleic acids for genetic testing. Both, the fetal cells and the cell-free fetal nucleic acids can be enriched from peripheral blood of pregnant women which is sampled from the cubital vain. As blood sampling is risk-free to pregnant women and their fetuses prenatal diagnosis based on non-invasive approaches would not be restricted to pregnant women at risk.

1.2.1 Cell-free fetal DNA and RNA

Cell-free fetal DNA (cffDNA) was first discovered by the group of Dennis Lo in 1997 (4). It originates from the syncytiotrophoblast. Cytotrophoblast cells fusing with the syncytiotrophoblast feed DNA into this syncytium. There, DNA is processed before being released into the maternal circulation. When this processed DNA was investigated by means of real-time PCR the main proportion of cffDNA turned out to be shorter than 0.3 kb, whereas maternal cell-free DNA, on average, was larger than 1.0 kb. Due to acceptable proportions of cffDNA in fractions less than 0.3 kb ranging from 22.2% to 87.1% (5), fetal sex and fetal

RhD status may be well investigated by the presence of Y-chromosome sequences and *RhD* genes (on chromosome 1) in *RhD*-negative women, respectively. Unlike these analyses of fetal sequences absent from maternal genome, the detection of single gene disorders (cystic fibrosis, β-thalassemia) and fetal trisomies (trisomy 21, trisomy 18, trisomy 13) is technically highly demanding. Strategies for discriminating fetal from maternal sequences both carrying the same mutation either use differences in DNA methylation (*maspin* gene, *RASSF1A*), single nucleotide polymorphisms (SNPs) or rely on circulating mRNA absent from maternal transcriptome such as placentally derived *PLAC4* mRNA (6-8). By the use of cffDNA NIPD has come true at least for the diagnosis of some paternally inherited single gene disorders, hemolytic disease of newborn, or families requiring prenatal fetal sex determination. However, analysis based on cffDNA currently does not allow for detecting mutations inherited from the maternal genome as this is true for X chromosome-linked and many recessive mutations. The use of tissue-specific mRNA may be an alternative approach for detecting fetal aneuploidy, but needs to be validated in clinical studies (9).

1.2.2 Circulating fetal cells

The discovery of fetal cells trafficking into maternal circulation dates back to 1893, when Gerog Schmorl, a German pathologist working on puerperal eclampsia, examined 17 bodies of deceased pregnant women affected with eclampsia (10, 11). In autopsied lung capillaries and – less frequently – in larger lung vessels he found thrombi that consisted of liver cells and big cells containing multiple nuclei. These multinucleated and giant cells were known to occur only in the uterus with the placenta and in the bone marrow. Schmorl correctly identified the multinucleated cells as deriving from the placenta. He ruled out bone marrow to be the source of these cells due to lack of ruptured vessels or macroscopic bleeding that would have given these cells access to the maternal circulation.

Almost a hundred years later, the emerging of new methods in molecular biology with PCR in 1983 probably being the most important, greatly influenced the everyday life in life science as DNA amplification was eased and caused PCR to be spread throughout the laboratories. This was also true for research in the field of NIPD that concentrated on the analysis of fetal cells present in maternal circulation

for the purpose of genetic diagnosis. NIPD based on these cells faces two main challenges, namely rarity and contamination.

Using fluorescence *in situ* hybridization (FISH) and primed *in situ* labeling (PRINS) Krabchi *et al.* determined the amount of circulating fetal cells in normal pregnancies at 18 to 22 weeks of gestation to range from two to six fetal cells per milliliter of maternal blood (12). Additionally, they found the number of circulating fetal cells to be three to five times higher in cases with trisomy 21 fetuses (13). Because of their scarcity, analysis of these cells always implicated the use of enrichment procedures to get rid of the vast majority of maternal cells. The protocols range from cell sorting based on immunological methods [fluorescence activated cell sorting (FACS), magnetic cell sorting (MACS)] to filtration by size exclusion and chip-based enrichment by means of microfluidics. First, FACS and then MACS was implemented by the research community to isolate fetal cells. FACS using DNA index values or monoclonal antibodies against the transferrin receptor (CD71) and glycophorin A (GPA) was performed for enrichment of erythroblasts that in turn were identified to be fetal by means of Y-FISH (14) or to be trisomic using chromosome 21 specific probes (15-17). MACS was performed for both positive and negative selection. For positive selection of trophoblast cells, antibodies against human leukocyte antigen G (HLA-G), human syncytiotrophoblast and non-villous cytotrophoblast cells were used (18, 19). Erythroblasts were either positively selected by MACS using antibodies against GPA, CD71, CD36, small-i and/or HAE9 (20-23) or selected by combining leukocyte depletion (anti-CD45 or anti-CD14 antibodies) with subsequent positive selection by means of anti-GPA and anti-CD71 antibodies (24, 25). For analysis these MACS-enriched cells were stained and forwarded to either FISH (18, 25) or PCR (19, 22, 24, 26). Hennerbichler *et al.* coupled cell sorting methods with further (virtual) enrichment by means of laser scanning microscopy (27). They used both immunofluorescence labeling and FISH on MACS pre-enriched cell suspensions. Fluorescent cells, which were automatically detected by means of laser scanning microscopy were relocated and checked for FISH signals.

Recently two new enrichment methods have shown up: filtration [isolation by size of epithelial tumor cells, (ISET)] (28) and microfluidics (29). The ISET filter contains pores of 8 µm in diameter and allows retaining cells bigger than that such as

trophoblast cells, whereas smaller cells (leucocytes, lymphocytes) may pass the pores of the filter. Erythrocytes are cleared from the blood samples before filtration by lysis treatment. Using ISET filter it has been shown that trophoblast cells can be enriched from peripheral blood of pregnant women, labeled on the filter by means of cytokeratin and analyzed using PCR of Y-chromosomal (Y-PCR) and short tandem repeats (STR) loci (30). The idea of using a microfluidic device has been recently introduced into fetal cell enrichment recently With this, Huang *et al.* obtained an erythrocyte reduction to approximately 0.01% from peripheral blood of non-pregnant individuals with ~ $5.0 \cdot 10^6$ erythrocytes remaining in the final suspension. Additionally, they were able to identify a mean of 37 nucleated red blood cells (NRBCs) per milliliter maternal blood with the trisomy 21 cases showing a mean of 51.81 cells per ml using this microfluidic approach in combination with a magnetic device for hemoglobin-based cell isolation, in all 58 (37 euploid and 21 aneuploid) surveyed cases of pregnancy (29). However, they did not test whether the detected NRBCs were of fetal origin. The identification of fetal cells in NIPD however still remains a critical step because all enrichment methods end up with cell fractions still containing a vast majority of maternal cells. This contamination with maternal cells makes fetal cell identification much more complicated because we lack a marker allowing to unambiguously discriminate fetal from maternal cells. Among the currently used methods for fetal cell detection only Y-FISH and immunostaining using an antibody against the epsilon chain of hemoglobin (Hbε) allows to label targets (molecules) absent from maternal cells. Despite their absence from maternal cells, these approaches face major drawbacks. Detection of Y chromosome sequences does not allow for detecting fetal cells originating from female fetuses. It has also been shown that Y-FISH is prone to yield false positive results (25). On the other hand, anti-Hbε antibodies label female and male early erythroblasts with a specificity of 100%. Unfortunately, early erythroblasts represent just a minor fraction of the circulating fetal cells and their frequency in peripheral blood of pregnant women is controversially discussed (31-35). Other targets such as gamma-chain of hemoglobin (Hbγ) are not specific to fetal erythroblasts as they were shown to be present also in maternal erythroblasts (36) and analysis without further identification may lead to false positive or false negative results. Thus,

current identification protocols need to link labeling techniques with molecular genetic or cytogenetic analysis for fetal cell identification and correct analysis. The labeling and molecular genetic or cytogenetic techniques allow several combinations.

1.2.2.1 No staining – identification via aneuploidy

An exception to the above stated approaches of combined staining and identification is to search for trisomic FISH or PRINS signals. The detection of trisomic nuclei includes both the identification of a fetal cell and the diagnosis of the respective trisomy. Furthermore, X and Y probes can be used for detecting male fetal cells and additional X and Y chromosomes. Most of these experiments were performed using cell lysis by means of Carnoy fixation followed by FISH analysis. These studies did not involve enrichment techniques other than cell lysis and therefore might be seen as the best estimates regarding the number of circulating fetal cells. Krabchi *et al.* published the number of circulating fetal cells ranging from two to six Y-positive cells per ml of maternal blood (12). This was confirmed by Mergenthaler *at al.* using a double-FISH technique yielding 12 to 20 XY-positive and Y-double-positive cells (two different Y chromosome probes) per ml of maternal blood (37). The number of circulating fetal cells in pregnancies affected with trisomic fetuses at gestational ages ranging from 13 to 22 weeks of gestation was shown to be higher than in normal pregnancies (13). Additionally to the estimations regarding the frequency of fetal cells circulating in maternal blood, several kinds of aneuploidy (47,XXX; 47,XXY; 47,XYY; 47,XY,+13; 47,XY,+18) and cases of triploidy (69,XXX) were also detected using the approach of Carnoy fixation and FISH or PRINS FISH (38). FISH and PRINS technique using 13, 18, 21, X and Y probes succeeded to detect male but not female and trisomic (triploidic) but not disomic fetal cells. Whereas the former apparently is not option for NIPD the latter is restricted to detect aneuploidy cases missing the detection of single gene disorders. Unfortunately, under rare cell conditions FISH is prone to false positive signals and precautions such as reverse XY FISH (33) or YY-FISH (37) need to be taken to exclude false positive results. However, not only XY-FISH is prone to false positive signals but also FISH using 13, 18 and 21 probes. Comparing cells enriched from three normal and three pathological pregnancies (with trisomy 13, 18, and 21 fetuses) I could confirm this by observing several split

signals especially with 18 probes (mimicking trisomy 18) and cells derived from normal pregnancies displaying trisomy 21 (data not shown).

1.2.2.2 Unspecific staining – identification via FISH or PCR

Another simple yet combined approach is to use relatively unspecific histochemical staining to identify erythroblasts based on morphology and to confirm fetal origin by means of FISH (for trisomic cells or Y chromosome) or PCR (Y chromosome sequences, STR loci or mutations). Half of the May-Gruenwald stained erythroblasts enriched from maternal circulation were shown to be of fetal origin using PCR of Y chromosomal and *RhD* gene sequences in *RhD*-negative women (22). However, PCR was successful in 42.2% (54 of 128) of the cases only. In another study, May-Gruenwald-Giemsa stained erythroblasts were microdissected and tested for ß-globin gene mutations by means of real-time PCR followed by 2plex PCR for the polymorphic markers D13S314 and GABRB3. PCR of polymorphic markers was successful in 57.1% (128 of 224 cells). Cells yielding PCR fragments could be allocated to either fetal or maternal origin in 37.5% of the cases whereas in 62.5% the PCR was uninformative due to homozygosity or allele drop out (ADO). Gene amplicons of ß-globin were achieved in 7% of the analyzed cells (16 of 224) only and resulted in correct diagnosis of fetal thalassemia status in two pregnancies at risk. This combined approach of unspecific staining and identification by means of FISH or PCR is restricted to the detection of (maternal and fetal) erythroblasts as this is the only target cell type, which can be morphologically identified. Erythroblasts have a short life span in maternal circulation. Thus, they are not likely to derive from earlier pregnancies as this was published to be true for fetal lymphocytes (39). On the other hand, the erythroblasts' nuclei are very compact and show signs of apoptosis resulting in low PCR and FISH efficiencies (40-42). These low efficiencies may also result from reagents used for staining. Methylene blue (reagent in May-Gruenwald staining solution) directly binds to DNA, may intercalate and cause helical unwinding (43). Furthermore, in conjunction with white light, singlet oxygen species are formed causing single-strand breaks and oxidative alterations of guanine residues (44, 45). This may support my findings that erythroblasts stained with May-Gruenwald but not with immunological methods devoid of methylene blue yielded both low PCR success and PCR efficiency (data not shown).

1.2.2.3 Immunological staining – identification via FISH and PCR

The use of immunologically-based staining methods allows to detect fetal cell types such as embryonic (early) and fetal erythroblasts as well as trophoblast cells. Furthermore, i-antigen and CD34 were used for cell labeling trying to get hold of fetal (31).

For erythroblasts labeling antibodies against the zeta (ζ), epsilon- (ε) or gamma-chain (γ) of hemoglobin and glycophorin A were used either separately or in combinations (27, 31-36, 46-49). PCR-based confirmation of the cells' identity was performed using either amelogenin (31, 34, 48), STR loci (47) or other polymorphisms (48). Sitar *et al.* (31) reported on the detection of 5 – 48 (28 ± 18) Hbε-positive erythroblasts from a total of 56 pregnancies (8th – 11th week of pregnancy) after performing non-physiological enrichment from 25 ml of peripheral blood. From 49 pregnancies at gestational ages ranging from 14 to 18 weeks they still detected 2 to 22 (15 ± 6) Hbε-positive erythroblasts. PCR analysis of 38 pregnancies yielded correct sex in 18 of 18 male and 19 of 20 female cases. One sample with XX karyotype (derived from invasive testing) showed to be male by means of sexing PCR. However, it was not clear from the manuscript whether PCR was done on Hb$^+$ cells. Another study performed by Nagy *et al.* support the comparatively high numbers of Hbε$^+$ cells. They found an average of 8.1 Hbε$^+$ cells (6 – 11) in all eight cases of pregnancies (10th – 14th weeks of gestation) and 3.0 Hbε$^+$ cells (0 – 7) in four of five pregnancies at gestational ages between the 22nd and 25th week of pregnancy (the latter group underwent AC in the 18th week of pregnancy). Single Hbε$^+$ cells were micromanipulated and forwarded to quantitative fluorescent PCR (QF-PCR) yielding concordant fetal sex with AC karyotyping in nine of ten cases. In one case QF-PCR failed to detect male sequences. Furthermore, Klinefelter Syndrome (XXY) was correctly detected in two of two cases from Hbε$^+$ cells. Two other studies targeted Hbγ (47) and GPA (48) in order to detect erythroblasts. Hbγ$^+$ cells were detected in all nine samples enriched by FACS. Applying a scoring system on every detected cell based on four parameters (nuclear roundness, nuclear morphology, cytoplasmatic Hbγ staining intensity and brightness; 0 to 3 points each) they were able to differentiate Hbγ$^+$ cells with cumulative scores ≥ 9 from cells yielding scores ≤ 5. Using fluorescent PCR of three STR loci (D21S1411, D21S11 and D18S535) they correctly identified

four cases of trisomy 21 fetuses and one case of a trisomy 18 fetus. The second study using GPA used primer extension preamplification (PEP) PCR to amplify amelogenin locus for sex determination. PCR of 107 cells (51.9%) was successful and yielded correct fetal sex identification in 65% of the cases(48).

Identification by means of FISH draws different picture of the frequency of circulating Hbε$^+$ cells. Investigating 48 pregnancies Mavrou *et al.* detected a mean of 9.2 Hbε$^+$ cells from 1° trimester (n = 26) and a mean of 4.2 Hbε$^+$ cells from 2° trimester (n = 22) pregnancies (20 ml each). With a mean of 22 cells the number of fetal (Hbε$^+$) cells was higher in pregnancies affected with trisomy 21 fetuses than compared to normal pregnancies. FISH using X, Y and chromosome 21 specific probes were successful in 24 of 29 cases. In four of four cases with trisomy 21 fetuses all Hbε$^+$ cells showed three signals for chromosome 21 (32). This finding is in contrast to results of other groups (25, 33, 35, 46). They report Hbε$^+$ cells to be very rare. Christensen *et al.* detected only one Hbε$^+$/Y$^+$ cell in 1 of 12 samples representing a total of 182 ml of maternal blood (35). In a later study they compared a 3-step enrichment method consisting of density gradient centrifugation, CD45/CD14 MACS depletion to a one-step CD71 positive selection of erythroblasts. Enriched cells were stained either with anti-ζ or anti-γ/anti-ε antibodies. True fetal origin was confirmed by reverse XY-FISH. Using the 3-step approach they could not detect a single fetal cell from 371 ml of peripheral blood of pregnant women whereas using the one-step method, two fetal cells were identified (25). Recently, they investigated 573 ml of peripheral blood and confirmed three cells (one Hbε$^+$ and two Hbζ$^+$) to be fetal using reverse XY-FISH. However, in the same study they also used hypotonic treatment, Carnoy fixation and reverse XY-FISH identifying 28 male nuclei from 15 ml of peripheral blood (33).

For trophoblast cell detection antibodies against HLA-G, KL1, placental alkaline phosphatase, placental growth factor, and neuroD2 were used (18, 30, 50). HLA-G (clone MEM-G/9) was used to determine the potential of clonal expansion of trophoblast cells. Guetta *et al.* detected a mean of 6.9 XY-positive cells per 20 ml of blood in the cultured samples originating from women carrying male fetuses. Compared to uncultured samples this represented a fivefold increase (18). Another group used the ISET filter method to isolate trophoblast cells deriving

from 13 pregnancies (11th – 12th week of gestation) (30). They found one to seven Y^+ cells in all six samples of mothers carrying male fetuses from as little as 2 ml of blood. None of the 26 cells isolated from mothers carrying female fetuses was Y^+. The data were confirmed using PCR of three STR loci (D16S3018, D16S3031 and D16S539). On the contrary, Tjoa *et al.* were not able to detect trophoblast cells from nine pregnancies (each 20 ml) with male fetuses at gestational ages ranging from 10 to 20 weeks of pregnancy (50). After labeling they found cells positive for HLA-G (clone 4H48) but negative for both placental growth factor and neuroD2. When confirming the cells' identities with XY-FISH, none of the HLA-G^+ cells turned out to be Y^+.

1.3 Minimally invasive prenatal diagnosis

Intact fetal cells may also be obtained from the uterine cavity and the endocervical canal either by transcervical mucus collection or intrauterine lavage (51-56). They may be collected between 5 – 7 and 13 – 15 weeks of gestation. The time window for collection of these cells ends in early second trimester when the uterine cavity disappears (57). Methods for collecting transcervical cells (TCC) include mucus aspiration or lavage (intrauterine lavage, IUL) of the endocervical canal using different devices such as cotton swabs, cytobrushes, and different cannulae, respectively (57). The first studies used Y chromosome and chromosome metaphase banding pattern to identify fetal cells and reported both false-positive and -negative results. This was thought to result from contamination by male spermatozoa, and so Adinolfi *et al.* used PRINS to detect trophoblast cells from TCC samples (58). In the following years it was shown that the percentage of TCC containing samples varied between 50% – 70% using aspirated mucus and 80% – 90% using the lavage method. The incidence of fetal cells detected by FISH were ranging from 0.5% to 40% (57). Recently, Cioni *et al.* compared mucus collection to IUL in 126 samples (51). Fetal sex was detected correctly in 56 of 56 (100%) female pregnancies by IUL. Y-PCR of collected mucus was positive in 3 of 56 female samples resulting in a correct female sexing in 53 of 56 cases (94.6%). Regarding the detection of male fetal cells from IUL samples Y-PCR and FISH correctly determined fetal sex in 55 of 67 cases (82%); mucus samples scored positive in 16 of 67 samples (23.9%) indication IUL to be superior to mucus collection. In 2007, a study on 181 IUL samples at 5 to 12 weeks of

gestation done by Bussani *et al.* isolated chorionic villous filaments or cell clumps of trophoblastic origin in 152 samples (84.8%). Using two different QF-PCR with a total of nine loci (amelogenin, D13S631, D13S634, D18D386, D18S535, D21S11, and D21S1411) they detected paternally derived alleles in all samples. Furthermore, they successfully detected two cases each of Turner Syndrome (45,X0) and Down Syndrome (47,+21).

1.4 Automated scanning

Imaging software highly facilitates cell detection in samples containing mixed cell populations especially under rare cell conditions. Visual detection of rare cells is cumbersome, needs trained personnel and is very time consuming The time for visual scanning of cells or nuclei on a slide is indirectly proportional to the signal size. This is quite obvious as smaller signals such as FISH spots long for objectives in higher magnification as bigger signals such as cytoplasmic staining. The three observers of Krabchi *et al.* for sure had a hard time visually checking 12 samples spread on 32 slides each using a magnification of 400x. On detecting nuclei containing two FISH spots in different colors (X, Y) they had to check the nucleus in 1000x magnification and document its image (12). In order to relief lab personnel from back breaking scanning image software was designed to automatically detect cells of interest by means of staining pattern.

Tanke *et al.* used an automated screening to detect Vector Blue labeled Hbγ^+ erythroblasts from 172 peripheral blood samples post CVS sampling and triple density gradient enrichment (59). They detected one positive cell among a million negative cells on a cytospin. The time to automatically analyze a whole slide was estimated to range between six and nine hours. Two years later the same group reported on the automated image processing of another 42 maternal samples (60). Again they used a triple density gradient to enrich the mononuclear cell fraction (MNC), labeled the cells using anti-Hbγ antibody (Vector Blue) and performed XY-FISH Automated scanning of 44 slides yielded 23 slides containing at least one Hbγ^+ cell (range: 1 – 111 cells), whereas manual screening of the same slides identified only 19 slides containing at least one Hbγ^+ cell (range 1 – 40 cells). The time needed for automated scanning was reported to range from 1 h 20 min to 7 h 20 min. Manual scanning, on average, took 10 – 45 min.

In 2000, Méhes *et al.* analyzed immunolabeled tumor cells in hematopoietic samples using MetaCyte (Metasystems, Germany), a fluorescence-based microscopic scanning system capable of relocating detected cells (61) achieving good correlation between manual and automated scanning of 57 images containing a total of 31500 cells (18 – 1,363 cells per image). Shortly after that, two different image analysis applications were used to detect fetal erythroblasts enriched from peripheral blood of pregnant women (35). Slides containing erythroblasts from fetal and maternal samples post CVS were labeled with anti-Hbγ/Vector Blue/DAPI/XY-FISH were scanned using a system capable of brightfield scanning (Vector Blue) combined with fluorescence image analysis for FISH (Applied Imaging). Fetal erythroblasts labeled with anti-Hbγ/FITC/DAPI/XY-FISH were forwarded to automated image analysis using RCDetect (MetaSystems). Regarding expenditure of time they found fluorescence-based scanning (12 min per slide) to be superior to brightfield-based scanning (30 min per slide).

Another approach to automatically detect male fetal cells was performed using Ikoniscope (Ikonisys Inc.) (62). A total of 12 samples was taken from pregnant women carrying male (n = 6) and female (n = 6) fetuses. Upon cell lysis and XY FISH, 18 slides (36000 scan fields) were scanned to detect nuclei showing XX and XY FISH signals, respectively. Using just one X and one Y FISH probe, XY-positive nuclei were not only found in all samples derived from women carrying male fetuses (range 3 to 53 positive nuclei) but also in samples from women carrying female fetuses (range 7 to 34 XY positive nuclei). After redesigning the study, they used one X chromosome along with two different Y chromosome probes and correctly detected XY-positive nuclei in all 4 samples derived from women carrying male fetuses (range two to six XY-positive nuclei per milliliter of sampled maternal blood) but not in samples from women carrying female fetuses. In a recently published paper they expanded their approach and combined Hbγ– and Hbε-fluorescence staining with XY FISH. Using XdY (X double Y) FISH only, they detected male nuclei in 27 of 29 cases of male pregnancies at an average of 0.8 and 0.4 male nuclei from 1° and 2° trimester pregnancies, respectively. No XY positive nudei were detected in two out of two female pregnancies. The same experimental settings were applied, when they implemented a density gradient

enrichment (1.083 g/dl) before FISH analysis. After scanning they found male nuclei in 28 of the 29 samples from male pregnancies, but also one XY-positive nucleus out of four female pregnancies. When combining XY-FISH method with anti-hemoglobin labeling (Hbγ and Hbε), they detected only one XY-positive cell out of 22 male pregnancies.

2 Aim

Non-invasive prenatal diagnosis based on circulating fetal cells is highly demanding because of the rarity of fetal cells circulating in the maternal blood and the contamination due to the high background of maternal cells in theanalyzed samples. Additionally, analysis needs to meet highest accuracy due to the possible impact of the analysis result.

As there is no marker capable of detecting all circulating fetal cells the objective of this work was to develop a method allowing for unambiguous and sex-independent detection and discrimination of cells sharing a haploid set of chromosomes as this is true for fetal and maternal cells.

3 Materials

Table 1: Consumables

Consumable	Company / reference number (provided by)
Multiplate 96 Biozym	Biozym Biotech Trading GmbH, Vienna, Austria / 621820 (ZMF I)
Adhesive PCR Film	VWR International GmbH, Vienna, Austria / 732-4949 (ZMF I)
AmpliGrid AG480F 1µl reaction slides	Olympus Life Science Research Europa GmbH, Munich, Germany / OAX04202
Cell strainer, 40µm Nylon	BD Falcon, Belgium / 352340
Cyto buckets	Andreas Hettich GmbH & Ko KG, Tuttlingen, Germany / 1665
Filter cards	VWR International GmbH, Vienna, Austria / HET-1676
Medicon, 35µm	Dako Österreich GmbH, Vienna, Austria / 79300S
Microscope cover glass, 18 x 18 mm	Marienfeld, Lauda-Königshofen, Germany / 0101030
MicroSlides, cleaned	Karl Hecht Ges.mbH, Fritzens, Austria / 2406
MiniMACS Separation Columns, type MS	Miltenyi Biotec GmbH, Bergisch Gladbach, Germany / 130-042-201
PEN-membrane Slides	Carl Zeiss MicroImaging, Munich, Germany / 1440-1000
Reaction tubes, 1.5ml	Eppendorf Austria GmbH, Vienna, Austria / 0030125150
Reaction tubes, 200µl	Biozym Biotech Trading GmbH, Vienna, Austria / 710920
Sample tubes	Drott Medizintechnik GmbH, Vienna, Austria / 202825
Slides, Superfrost Plus	Gerhard Menzel Glasbearbeitungswerk GmbH & Co KG, Braunschweig, Germany / J1800AMNZ
Tips, 0.1 - 10µl, ep Dual filter tips	Eppendorf Austria GmbH, Vienna, Austria / 0030077504
Tips, 2 - 200µl, ep Dual filter tips	Eppendorf Austria GmbH, Vienna, Austria / 0030077555
Tips, 50 - 1000µl, ep Dual filter tips	Eppendorf Austria GmbH, Vienna, Austria / 0030077571
Tubes, 15ml	Bertoni, Vienna, Austria / 2323-015
Tubes, 50ml	Bertoni, Vienna, Austria / 2343-050

Table 2: Antibodies

Antibody	Company / reference number (provided by)
anti-Hb-epsilon	Europa Bioproducts Ltd., Cambridge, UK / CR8008M1
anti-Hb-gamma	Europa Bioproducts Ltd., Cambridge, UK / CR8115M1
anti-Hb-gamma, FITC labeled	Europa Bioproducts Ltd., Cambridge, UK / CR8115M1F
CD71 MicroBeads	Miltenyi Biotec GmbH, Bergisch Gladbach, Germany / 130-046-210
GZ112 antibody	Dr. Michaele Hartmann, Institute for Cell Biology, Histology & Embryology, Medical University Graz, Austria
GZ158 antibody	Dr. Michaele Hartmann, Institute for Cell Biology, Histology & Embryology, Medical University Graz, Austria
polyclonal goat anti-mouse IgG/FITC; goat $F(ab')_2$	Dako Österreich GmbH, Vienna, Austria / F0479

Table 3: Reagents, solutions, buffers and media

Reagents/solutions/buffers/media	Company/reference number (provided by)
Albumin, bovine fraction V powder	Sigma-Aldrich Handels GmbH, Vienna, Austria / A2153-50G
AmpliTaq Gold DNA Polymerase	Applied Biosystems Austria GmbH, Brunn am Gebirge, Austria / 4311806
Citric acid monohydrate	Merck GesmbH, Vienna, Austria / 9651127
Dextrose anhydrous	Mallinckrodt Baker Inc., NJ, USA / 4912
Di-sodium phosphate dodecahydrate	Merck GesmbH, Vienna, Austria / 1.06579.1000
Ethylenediaminetetraacetic acid tetrasodium salt dihydrate (EDTA)	Sigma-Aldrich Handels GmbH, Vienna, Austria / ED4SS
Hank's buffered salt solution	Sigma-Aldrich Handels GmbH,Vienna, Austria / H4641
Histopaque 1077	Sigma-Aldrich Handels GmbH, Vienna, Austria / 10771-6X100ML
Histopaque 1083	Sigma-Aldrich Handels GmbH, Vienna, Austria / 10831-6X100ML
Human AB serum	University Clinic of Blood Group Serology and Transfusion Medicine, Medical University Graz, Austria
Hydrochloric acid (37%)	Merck GesmbH, Vienna, Austria / 1003172510
ILS 600	Promega GmbH, Mannhein, Germany / DG1071
May-Gruenwald's Eosin-Methylene Blue Solution, modified	Merck GesmbH, Vienna, Austria / 1.01424.0500
Medium 199 with Earl's Salts	Med Pro Vertrieb für medizinisch-diagnostische Produkte GmbH, Vienna, Austria / F0613
Poly-*L*-lysine	Sigma-Aldrich Handels GmbH, Vienna, Austria / P8920-100ML
Potassium dihydrogen phosphate	Merck GesmbH, Vienna, Austria / 1.04873.0250
Reference solution 290mOsm	Drott Medizintechnik GmbH, Vienna, Austria / 3MA029
Sodium chloride	Merck GesmbH, Vienna, Austria / 1.06404.1000
Sodium hydroxide	Merck GesmbH, Vienna, Austria / 1.06469.1000
TO-PRO-3 iodide	Invitrogen GmbH, Lofer, Austria / T3605
Tri-sodium citrate dehydrate	Merck GesmbH, Vienna, Austria / 1.06448.0500
Trypan Blue Solution (0.4%)	Sigma-Aldrich Handels GmbH, Vienna, Austria / T8154
VectaShield Mounting Medium	Szabo-Scandic HandelsgmbH & Co KG, Vienna, Austria / H-1000

Table 4: Kits

Kit	Company/reference number (provided by)
AEC + Substrat Chromogen	Dako Österreich GmbH, Vienna, Austria / K3469
Antibody Diluent with Background Reducing Components	Dako Österreich GmbH, Vienna, Austria / S3022
Cell Extraction Kit	Olympus Life Science Research Europa GmbH, Munich, Germany / OAX04523
Fix&Perm	Szabo-Scandic HandelsgmbH & Co KG, Vienna, Austria / GAS002
PowerPlex 16 System	Promega GmbH, Mannhein, Germany / DC6531
UltraVision LP Large Volume Detection System HRP Polymer (Ready-To-Use)	Thermo Fisher Scientific, Cheshire, UK / TL060-HL
Wizard SV Gel & PCR Clean-Up System	Promega GmbH, Mannhein, Germany / A9282

Table 5: Tissues and cell lines

Tissue/cell line	Company / reference number (provided by)
Fractions enriched for erythroblasts	University Clinic of Obstetrics and Gynecology, Graz, Austria
Fractions enriched for trophoblasts	University Clinic of Obstetrics and Gynecology, Graz, Austria
Interruption tissues (villous trophoblasts, decidua)	Dr. Jansen, general practitioner, Graz, Austria
JAR choriocarcinoma cell line, HB-144	Dr. Esther Guetta, Danek Gertner Institute of Human Genetics, Tel Hashomer, Israel

Table 6: Software

Software	Company (provioded by)
GeneMapper 4.0	Applied Biosystems Austria GmbH, Brunn am Gebirge, Austria (ZMF I)
MetaferP V 3.2.129 RCDetect module	MetaSystems GmbH, Altlussheim, Germany
PALMRobo Software version 3.0.0.9	Carl Zeiss MicroImaging, Munich, Germany

Table 7: Equipment

Equipment	Company (provided by)
3730 DNA Analyzer	Applied Biosystems Austria GmbH, Brunn am Gebirge, Austria (ZMF I)
AmpliSpeed ASC400D, slide cycler	Olympus Life Science Research Europa GmbH, Munich, Germany
Axiovert M200	Carl Zeiss GmbH, Vienna, Austria
Biohit e10, pipette	Biohit Deutschland GmbH, Rosbach v. d. Höhe, Germany
Centrifuge, Beckman Allegra 6R Centrifuge	Werfen Austria, Vienna, Austria
Centrifuge, Biofuge pico	VWR International GmbH, Vienna, Austria
Cytocentrifuge, Universal 32, type 1605	Andreas Hettich GmbH & Ko KG, Tuttlingen, Germany
DNA Engine Dyad Peltier Thermal Cycler	Bio-Rad Laboratories GmbH, Vienna, Austria
Filter sets FS 01 (advanced), FS 17 (basic), FS 20, FS 26)	Carl Zeiss GmbH, Vienna, Austria
MACS MultiStand	Miltenyi Biotec GmbH, Bergisch Gladbach, Germany
Medimachine	Dako Österreich GmbH, Vienna, Austria
MiniMACS Separation Unit	Miltenyi Biotec GmbH, Bergisch Gladbach, Germany
MiniMACS Separator	Miltenyi Biotec GmbH, Bergisch Gladbach, Germany
Multipette stream	Eppendorf Austria GmbH, Vienna, Austria
Orion 3-Star Benchtop pH Meter	Bartelt GmbH, Graz, Austria
Osmometer, Fiske Advanced 2400	Drott Medizintechnik GmbH, Vienna, Austria (Institute for Physiology, Medical University Graz, Austria)
Thermomixer 5436	Eppendorf Austria GmbH, Vienna, Austria
Equipment	Company (provided by)
Ultraviolet Sterilizing PCR Workstation	Ltf Labortechnik GmbH & Co. KG, Wasserburg/B, Germany

4 Methods

4.1 Ethics

This PhD thesis was approved by the Ethics Committee of the Medical University of Graz, Austria (# 16-187 ex 04/05) and Sheba Medical Center's Ethics Board (Israel, Exp.# 97426). Informed consent was obtained from all subjects, according to the World Medical Association Declaration of Helsinki.

4.2 Basic protocols

For basic protocols of density gradient centrifugation, MACS enrichment, cytocentrifugation and labeling techniques such as histochemical staining, direct and indirect immunofluorescence labeling see section 7.

4.3 Antibodies used for enrichment and staining purposes

For enrichment and labeling of trophoblast cells mouse monoclonal antibodies GZ112 (63) and GZ158 were used. GZ158 was generated from a fusion of myeloma cells (P3NS1-Ag4-1) with spleen cells from a BALB/c mouse immunized with homogenized Jeg-3 (human choriocarcinoma) cells following the method of Goding (64). Using immunohistochemistry, supernatants binding pattern were investigated on frozen sections of first trimester placenta and decidua (trophoblast) (Figure 1) as well as on PBMNC cytospins (negative control) from a healthy individual (not shown). In addition, FACS analysis was performed on first trimester trophoblast cell fractions (purity of 90%) (65) to elucidate localization of the antibodies (Figure 2). Some of those identified as cell surface binding antibodies were then produced at larger scale and purified (BioGenes, Berlin, Germany). Immunocytochemical staining (sections 7.3.2 and 7.3.3) using GZ112 and GZ158 were performed at final concentrations of 2.24 µg/ml and 2.76 µg/ml, respectively.

Anti-Hbγ and anti-Hbε antibodies (Europa Bioproducts, Ely, UK) used for labeling erythroblast as well as FITC-labeled goat-anti-mouse F(ab')$_2$ antibody (DAKO, Austria) were used at 5 µg/ml. In some experiments we applied directly labeled anti-Hbγ-FITC (Europa Bioproducts)

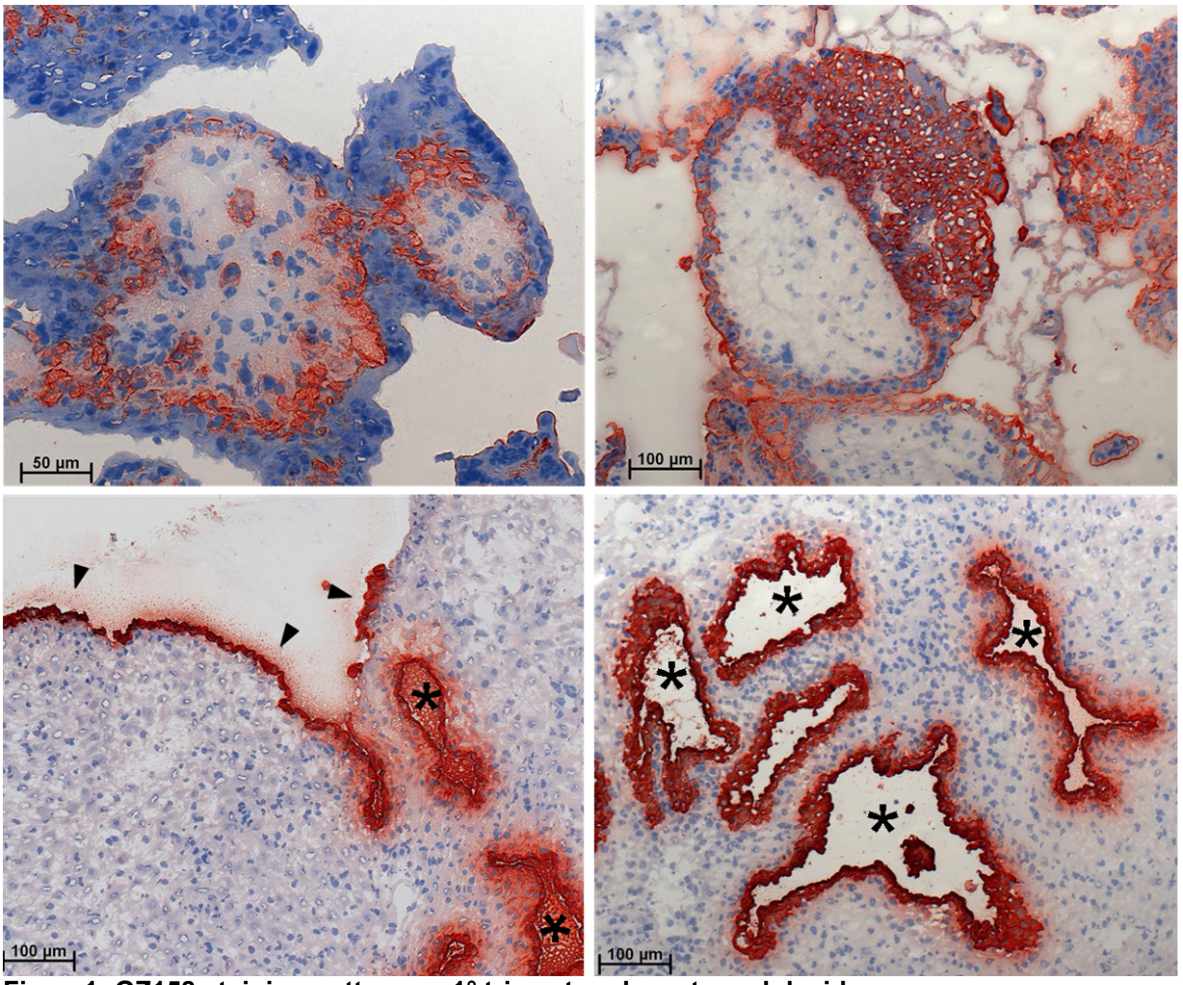

Figure1: GZ158 staining pattern on 1° trimester placenta and decidua
Frozen sections of villous (top) and decidual (bottom) tissues from termination of pregnancy (9th week of gestation) were stained using the antibody GZ158. For immunohistochemistry UltraVision LP Value Large Volume Detection System HRP Polymer (LabVision) was used together with AEC (DakoCytomation). GZ158 brightly stains villous cytotrophoblast cells (top left) as well as syncytiotrophoblast (top right). On sections of decidual tissues GZ158 stains epithelial cell layer (triangle, bottom left) and glands (asterisks, bottom)
(Immunohistology: Christine Daxböck)

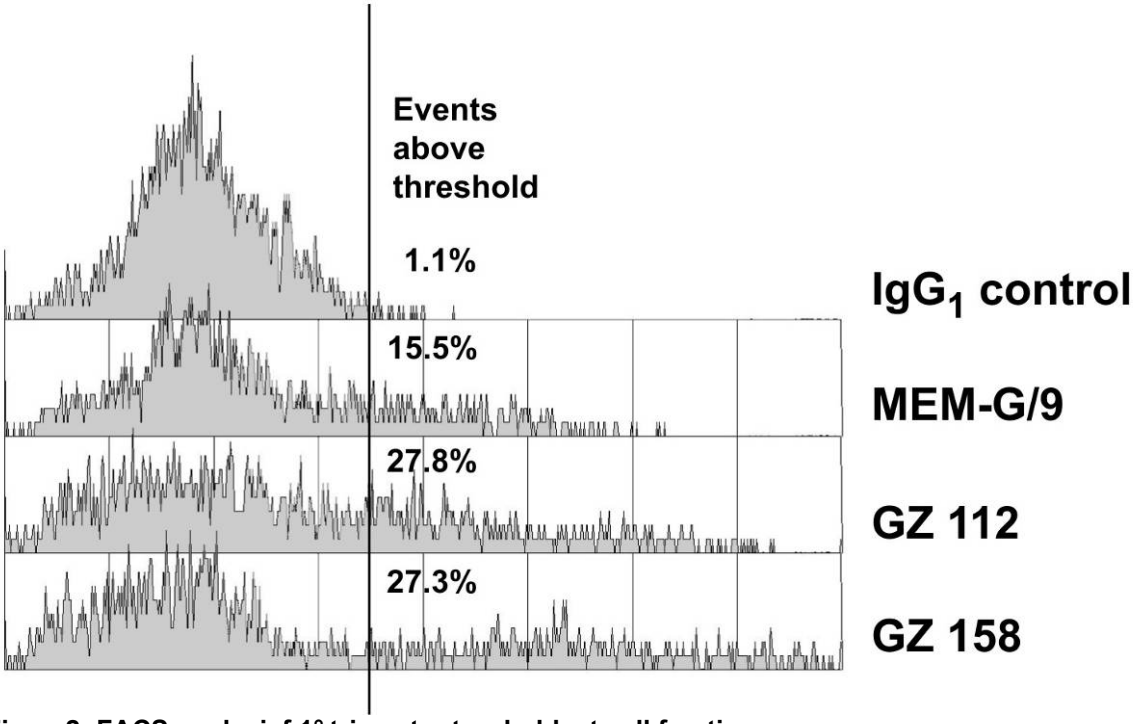

Figure2: FACS analysis of 1° trimester trophoblast cell fraction
In FACS analysis, GZ158 and GZ112 turned out to bind to the cells surface. The data were confirmed by an IgG_1 negative control and MEM-G/9 positive control antibodies. The latter is known to bind to HLA-G located on the cell surface
(FACS analysis: Mag. Dr. Kristina Kofler)

4.4 Cell sampling from cord blood

Cord blood was used as a source for fetal (Hbγ-positive) erythroblast enrichment. Cord blood samples were collected into EDTA tubes shortly after birth from deliveries occurring during night shift at the University Clinic of Obstetrics and Gynecology, Medical University of Graz, and stored at 4– 8 °C until further sampling the next day. Density gradient centrifugation was performed as described in the appendix (section 7.1.2). In some experimental settings low percentage of erythroblasts among the mononuclear cell (MNC) fraction was appreciated. In these cases the MNC fraction was cytocentrifuged onto glass slides according to the basic cytocentrifugation protocol (section 7.2). In experiments where high erythroblast percentages were necessary the MNC fraction was forwarded to MACS enrichment (section 7.1.4) using CD71-MicroBeads binding to transferrin receptor. This receptor is highly expressed on erythroblast cell surfaces that need to interact with the iron binding protein transferrin in order to enable iron up-take. Upon elution from MACS columns cytocentrifugation was performed as described (section 7.2).

4.5 Cell sampling from chorionic villous and decidual tissues

Chorionic villous and decidual tissues were obtained after terminations of pregnancies and forwarded to either mechanical or enzymatic treatment. Mechanically processed samples were used for molecular genetic analysis of fetal erythroblasts, trophoblast cells (chorionic villi), and maternal cells (decidual tissues), whereas enzymatic sampling was used to enrich trophoblast cells (chorionic villi) in order to establish classifier settings of the RCDetect cell scanning software

4.5.1 Mechanical digestion

Chorionic villi and decidual tissue pieces derived from first trimester interruption material were rinsed in PBS, separated under optical control and mechanically disaggregated using a MediMachine system (DAKO, Austria) according to the manufacturer's recommendations. In short, tissues were cut into pieces and transferred to a disintegration device called Medicon pre-conditioned with MACS buffer. The tissues were mechanically digested for 30 to 60 seconds through 40 µm pores, recovered from the device and filtered through a 40 µm nylon filter (Falcon, BD, Belgium). Cell suspensions were counted and cytocentrifuged onto membrane slides as described (section 7.2).

4.5.2 Enzymatic digestion

Enriched trophoblast cell or erythroblast fractions after enzymatic digestion of first trimester chorionic villi were provided by the University Clinic of Obstetrics and Gynecology. Tissues derived from termination of pregnancy were stored in Medium 199/DMEM/OP TINEM (500 ml / 500 ml / 0.75 mg) and villous trees were selected under optical control, rinsed in PBS and cut using a sterile scalpel. Thereafter the tissue pieces were transferred to cell culture flasks and digested using a mixture of 15 ml of Dispase/DNase and 15 ml of 0.25% Trypsin at 37 °C for 15 minutes. Following the first digest supernatants were separated from residual tissues which were digested again. Supernatants from both digests were pooled and washed twice in DMEM. The pellets were resuspended in 5 ml of DMEM and layered upon a density gradient prepared from mixtures of Percoll/10x HBSS (4 ml of 10x HBSS added to 36 ml of Percoll) and 1x HBSS solutions as shown in Table 8.

Table 8: Density gradient used for erythroblast or trophoblast cell enrichment
Density gradients were prepared from solutions 1 to 7 each containing a mixture of Percoll/10x HBSS and 1x HBSS. Immediately after preparation, the cell suspensions were loaded onto the gradient and centrifuged.

Layer	Percoll/10x HBSS [ml]	1x HBSS [ml]
1	3.5	1.5
2	3.0	2.0
3	2.5	2.5
4	2.0	3.0
5	1.5	3.5
6	1.0	4.0
7	0.5	4.5

Upon centrifugation buffy coat cells were collected from the interphase between the 6th and 7th layers, transferred to our lab and washed twice in MACS buffer before cytocentrifugation (section 7.2).

4.6 Artificial mixtures of JAR choriocarcinoma cells and peripheral blood mononuclear cells (PBMNCs)

Cells from human Y chromosome positive JAR choriocarcinoma cell line (American Tissue Type Collection, HB-144) were cultured and mixed with PBMNCs from non-pregnant healthy donors at the Danek Gertner Institute of Human Genetics (Tel-Hashomer, Israel) in order to establish artificial mixtures of non-related individuals as follows. JAR cells were cultured at 37°C in a humidified atmosphere of 5% CO_2 for seven days using RPMI 1640 medium (Biological Industries, Israel) supplemented with 10% FBS (Biological Industries), 2mM *L*-glutamine (Biological Industries) and 1% penicillin/streptomycin (Biological Industries). Blood samples from three non-pregnant women were drawn and PBMNC fraction was collected after single density gradient (1.077 g/ml) centrifugation at 1000x g at room temperature for 20 min.

From each sample, $1.5 \cdot 10^7$ PBMNC were then mixed with 1500 JAR cells, resulting in a quantitative relation of 10^4:1. The cell preparation was incubated with the antibody GZ158 (final concentration 96 µg/ml in PBS containing 0.1% BSA) for 30 min. After washing the cells with 500 µl of MACS buffer, the pellet was incubated for 30 min with 200 µl of FITC-labeled donkey-anti mouse F(ab')2 (1:50 in PBS/0.1% BSA; Jackson Immuno Research Europe, Suffolk, UK), washed and resuspended in 20µl of anti-FITC magnetic beads (Miltenyi Biotec) diluted in

80 µl of MACS buffer. Following incubation on a shaker at 4 °C for 15 min and another washing step, the cells were resuspended in 500 µl of MACS buffer and loaded onto a MiniMACS column (Miltenyi Biotec). MACS-positive cells were eluted according to the manufacturer's protocol. Approximately $4 \cdot 10^4$ of the positive cells were loaded onto eight PEN-membrane coated class slides (Carl Zeiss MicroImaging, Germany) using cytocentrifugation. The cells on the slides were fixed in 1% formaldehyde (Sigma Aldrich) or methanol for 15 min respectively and rinsed twice in PBS for 5 min. The air-dried slides were then shipped to Austria where nuclei were counterstained with 2 µM of the monomeric cyanine nucleic acid stain TO-PRO-3 (Invitrogen, Lofer, Austria) in PBS for 10 min and mounted in VectaShield (Szabo-Scandic Handelsgmbh & Co KG, Vienna, Austria). The slides were stored in the dark at room temperature before automated cell detection.

4.7 Automated rare cell detection

Metafer P RCDetect module (MetaSystems GmbH, Altlussheim, Germany) a special scanning system adapted to the laser microdissection system from PALM (Carl Zeiss MicroImaging,) was used to link automated cell detection with subsequent laser microdissection. In principle, this detection is based on immunofluorescence double labeling and morphology of cells in which negative cells show nucleic staining only. Double-labeled positive "candidate" cells additionally show a cytoplasmatic or surface staining and are therefore recognized as positive events if they meet a certain predefined set of parameter, called the classifier Thus, RCDetect, the rare cell detection software of Metafer P, was first trained on finding candidate cells resulting in the development of a classifier. Thereafter this classifier was used for rare cell detection

4.7.1 Training RCDetect software

RCDetect software was trained to recognize fetal candidate cells in two steps. First erythroblasts enriched from both cord blood and first trimester chorionic villi were subject to the establishment of classifiers. Then the classifier was further improved by using cells of other cell types such as JAR cells (choriocarcinoma cell line). Classifier development was done following the MetaSystems Finder Manual version 2.8.0 (MetaSystems). In short, slides containing FITC/TO-PRO-3 double

labeled cells were inserted onto the microscope stage and RCDetect software was started. A new classifier was created by using an existing classifier (supplemented with the software) to read the initial settings. Thereafter training images containing few positive cells and/or artifacts were captured from the inserted slides. In some cases, images originating from different slides were merged to create a "virtual" slide suited for classifier development. In the next step, FITC/TO-PRO-3 positive cells within these training images were defined as positive objects and non-cellular double labeled objects were defined as artifacts. Following that, RCDetect training was performed as follows. The training images were automatically analyzed using seven parameters, five designed for cell detection and two for cell selection. All parameters were given a maximum and a minimum value as well as a step size. Then the system used all possible combinations of these values to analyze the training images and listed the calculated error rates (false positive and false negative events) together with the respective parameter values. The parameter settings of the best fit were used to redefine the maximum and minimum values of the parameters and the iterations were repeated with reduced step sizes. After a third round of iteration, the parameter settings were stored and implemented into the classifier.

4.7.2 Rare cell detection

Slides containing cells labeled by immunofluorescence (IF) were inserted into the slide holder at the microscope stage and RCDetect was started using the appropriate classifier for cell detection. Coordinates of positive events were recorded during the scan and its images displayed in the image gallery. After the scan the image gallery was checked for positive cells. By using the coordinates of these events the cells were relocated for the purpose of harvesting by means of laser microdissection and pressure catapulting.

4.8 Lase microdissection and pressure catapulting (LMPC)

In order to collect single cells or cell pools the respective cells were cytocentrifuged onto PEN-membrane coated slides (Carl Zeiss MicroImaging). Post labeling (section 7.3) and semi-automated detection (4.7.2); the slides were rinsed in coplin jars to remove the cover glasses using PBS. Upon additional washing steps the slides were reinserted in the microscope stage and cells selected from the

RCDetect image gallery were relocated. For collecting the cells, reaction sites (anchors) of AmpliGrid slides were charged with 1µl of nuclease-free water and placed up-side-down on the membrane slide. To implement this protocol step into the process, I have developed a device to avoid the contact between collecting droplet and sample (section 5.2 and Figure 10). Using this device collecting droplets could be positioned above the candidate cells. Following this the cells were microdissected and catapulted using LMPC settings as indicated in Table 9. Upon catapulting the collection droplet was allowed to evaporate and the anchors were checked for presence of microdissectates.

Table 9: Laser Microdissection and Pressure Catapulting settings

	Microdissection	Pressure Catapulting
Objective	40x	40x
Laser Energy [%]	60 - 66	+18*
Laser focus	Focus plane (membrane)	-3µm*

*(delta to microdissection setting)

4.9 Low-volume on-chip cell lysis and multiplex-PCR

After microdissection the cells were forwarded to cell lysis (using Cell Extraction Kit, Olympus Life Science Research Europa) and subsequent multiplex-PCR (PowerPlex 16 System, Promega). All protocol steps were performed with equipment used only for this purpose. Precautions were taken to reduce contamination to a minimum: AmpliGrids were transferred to a PCR Workstation (UVP, UK). This PCR Workstation was restricted to pooled single and single cell PCR handling only. Sampling was done with a set of pipettes used for this purpose only.

4.9.1 Cell lysis

Reaction sites containing microdissected cell pools or single cells, negative controls (water) or positive controls (Standard DNA template 9947A, Promega) were charged with 0.75 µl of cell lysis mix (see Table 10) and immediately afterwards overlaid by 5 µl of sealing solution (Olympus Life Science Research Europa). Cell lysis was performed on a slide cycler (AmpliSpeed, Olympus Life Science Research Europa) at 75°C for 5 min followed by a 3 min inactivation step.

4.9.2 Multiplex-PCR

0.75 µl of PCR mix (see Table 10) was placed on top of the sealing solution. Due to physical properties of both aqueous PCR mix and sealing solution, the former passed through the latter and merged with cell lysate resulting in 1.5 µl reaction volume. Upon that DNA was amplified according to the manufacturer's recommendations (Technical Manual; PowerPlex 16 System, Promega). For details see Table 11. Following amplification the PCR fragments were either stored on-chip O/N or directly forwarded to PCR purification.

Table 10: Cell lysis and PCR mixes (for 30 reactions)

Protocol	Cell Lysis Mix (30 reactions)	Multiplex-PCR Mix (30 reactions)
Water [µl]	19.88	12.06
10x Cell Lysis Buffer [µl]	2.25	-
Lysis Enzyme [µl]	0.37	-
Gold Star 10x Buffer [µl]	-	4.5
PowerPlex 16 10x Primer Pair Mix [µl]	-	4.5
AmpliTaq Gold DNA Polymerase [µl]	-	1.44
Total Volume [µl]	22.5	22.5
Volume per Reaction [µl]	0.75	0.75

Table 11: PowerPlex 16 System amplification protocol (TSC400D SlideCycler)

Cycles	Temperature	Time
1	95 °C	11 min
1	96 °C	1 min
10	94 °C	30 s
	94 °C – 60 °C	0.5 °C/s
	60 °C	1 min
	60 °C – 70 °C	0.3 °C/s
	70 °C	45 s
20	90 °C	30 s
	9 0°C – 60 °C	0.5 °C/s
	60 °C	1 min
	60 °C – 70 °C	0.3 °C/s
	70 °C	45 s
1	60 °C	30 min

4.10 Purification of PCR fragments

After amplification both PCR and sealing solutions were recovered from the AmpliGrid and purified using the Wizard Gel & PCR Clean-up System kit (Promega) according to the manufacturer's recommendations. Purified PCR fragments were eluted from columns using 32µl of RNase and DNase free water supplemented with the kit. The samples were either used for analysis by means of capillary electrophoresis or stored at -20 °C.

4.11 Fragment analysis

Approximately 15 µl of purified PCR samples were added to wells on a 96 well plate containing 4.7 µl of water and 0.3 µl of internal lane standard 600 (ILS 600) in each well. The samples were denaturized at 96 °C in a conventional cycler (DNA Engine Dyad Peltier Thermal cycler, Bio-Rad Laboratories GmbH, Vienna, Austria) for 3 min, cooled on ice immediately afterwards, and fed into a 3730 DNA Analyzer (Applied Biosystems Austria GmbH, Brunn am Gebirge, Austria) located at the Core Facility Molecular Biology (Center for Medical Research, Graz, Austria).

Electropherograms were analyzed with GeneMapper 4.0 (ABI Austria) to assign STR repeat numbers to detected peaks.

4.12 PCR efficiency and DNA profiles

DNA Profiles of each sampletype (JAR choriocarcinoma cell profile, PBMNC profiles of different donor individuals, fetal and maternal DNA profiles from termination of pregnancy tissues, DNA profile of the experimenter [operator]) were assessed by combining all DNA profiles from one and the same sample. PCR yielding at least one amplification product ("successful PCR") were included in the analysis. Lack of PCR fragments at single heterozygous or homozygous loci (no call) was defined as "amplification failure". This amplification failure was calculated from the number of failed loci divided by the total number of loci. ADO and heterozygous patterns were calculated from the results given by heterozygous loci only. Allele drop out (ADI) was defined as extra PCR fragments that either did not match both respective PCR profiles or matched the other (PBMNC or JAR, maternal or fetal) profile in cases where contamination was unlikely (single cell PCR). ADI was also calculated from heterozygous and homozygous loci. PCR

efficiency is expressed as successfully amplified alleles at heterozygous loci based on the theoretically maximal number of PCR fragments at heterozygous loci.

5 Results

5.1 Development of a classifier for multi cell type detection

5.1.1 Basic classifier

The first classifier was developed on fetal erythroblasts enriched from cord blood as described in section 4.4 and cytocentrifuged onto glass slides (section 7.2). The cells were stained on the slide using directly labeled anti-Hbγ/FITC antibody and TO-PRO-3, respectively, following the protocol described in section 7.3.2. Immediately after mounting, the slide was inserted onto the stage and scanned in order to retrieve training data. Of these training data, 15 fields containing a total of 14 erythroblasts were chosen for classifier development (Figure 3).

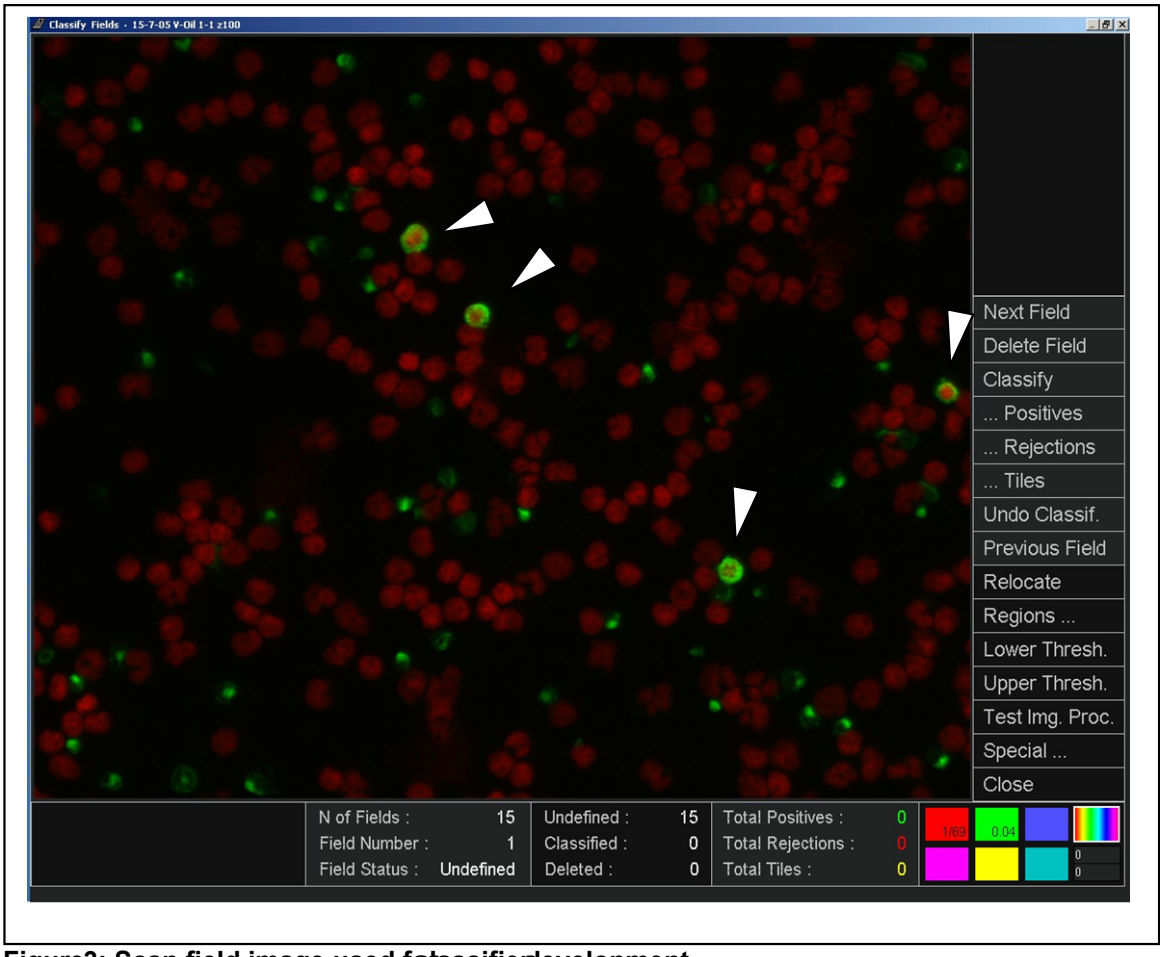

Figure 3: Scan field image used for classifier development
Fetal erythroblasts were enriched from cord blood and stained using directly FITC-labeled anti-Hbγ antibody and TO-PRO-3 nucleic counterstain. Training images were retrieved by scanning the slide in FITC (Hbγ) and Cy5 (TO-PRO-3) channels. RCDetect software was trained on 15 training field images containing a total of 14 FITC$^+$/TO-PRO-3$^+$ cells (white rectangles).

Error rates regarding false negative and false positive events were automatically assessed by RCDetect software (section 4.7.1). The parameter settings fitting best were stored as classifier "18-07-05 z200" (Figure 4).

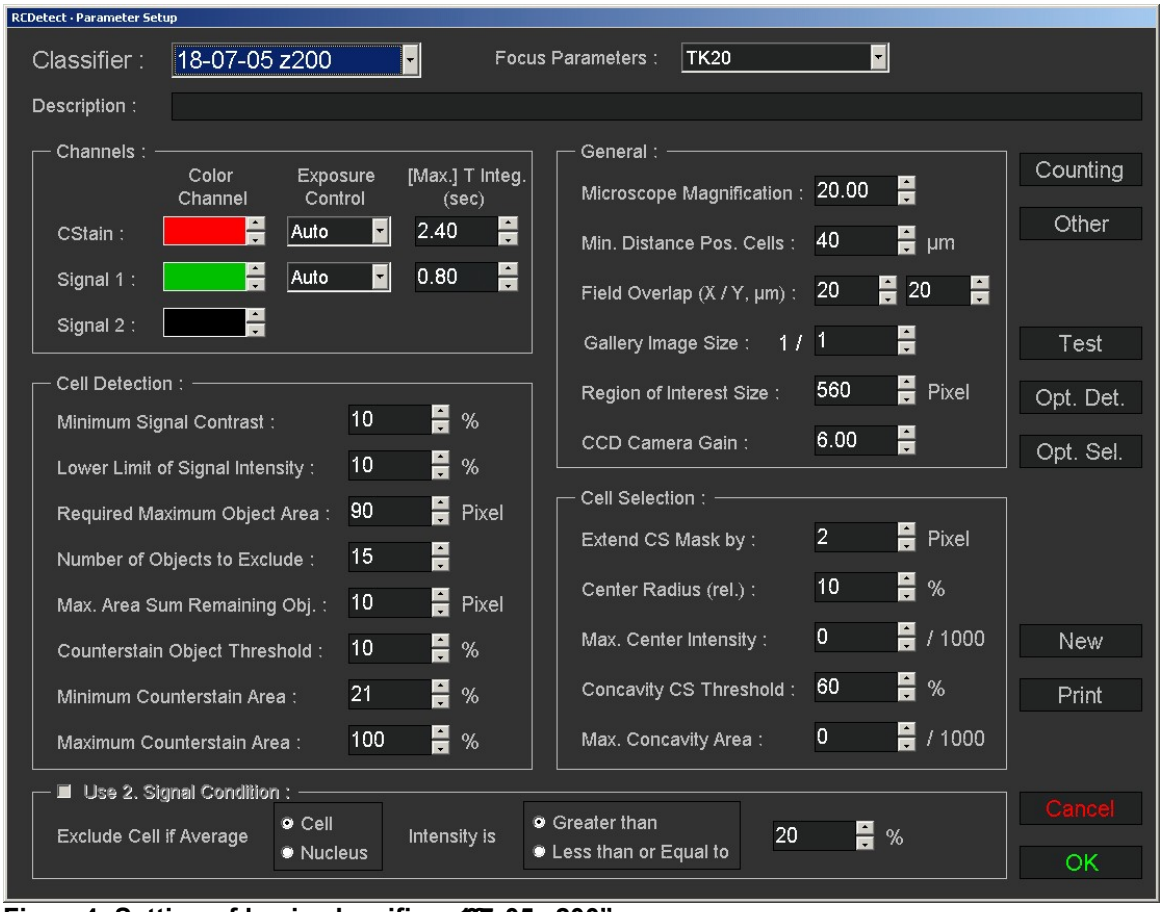

Figure 4: Setting of basic classifier „18-07-05 z200"
The values from the preceding iteration process done by RCDetect software that showed the lowest error rates for false positive and false negative events were transferred to the RCDetect parameter set up (Cell Detection box) and stored as classifier "18-07-05 z200". Further information on parameter settings are given in boxes "Channels" and "General": Maximum time of integration 0.8 sec (Signal 1: FITC channel) and 2.4 sec (CStain: TO-PRO-3); 20x objective (Microscope Magnification); 20 µm scan field overlap (Field Overlap)

5.1.2 Classifier optimization

Different parameter were optimized to meet the detection criteria of both, varying IF staining pattern caused by different cell types such as fetal (Hb^-) and embryonic (early) erythroblasts (Hb^+), trophoblast cells [(GZ158/ GZ112)$^+$] and JAR choriocarcinoma cells (GZ158$^-$) and varying IF intensities (Figure 5). Most of the adaptations to the first classifier concerned the following parameters: (a) the Maximum Integration Time ($I_{t,max}$; range: 0.2 – 2.4 seconds) during IF detecting of TO-PRO-3 and FITC signals (Cy5 and FITC channel, respectively) causing false positive ($I_{t,max}$ too long) or false negative ($I_{t,max}$ too short) events; (b) the Minimal Signal Contrast limiting detection areas (range: 10– 20% of the maximum possible

contrast of 255) as well as the Lower Limit of Signal Intensity excluding weakly stained cells from analysis (range 10 – 20% of the maximum signal intensity of the image) and (c) the Minimal Distance Positive Objects (range 10 – 20 µm) in combination with Field Overlap (X/Y) (range: 20 – 113 µm / 20 – 144 µm) influencing cell detecting and cell counting of positive adjacent events and events located at the border of scan fields. However, the probably biggest improvement was achieved when I switched from 20x objective to 10x objective for scanning the slides. Changing Magnification from 20x to 10x reduced the number of scan fields of a 120 mm^2 cytospin from 1623 to 271. Although scanning time per field nearly was doubled, the total scanning time could be cut to one-third so that $1 \cdot 10^5$ cells (standard cytocentrifugation area: 20 mm^2) were scanned in approximately 20 minutes (Figure 6).

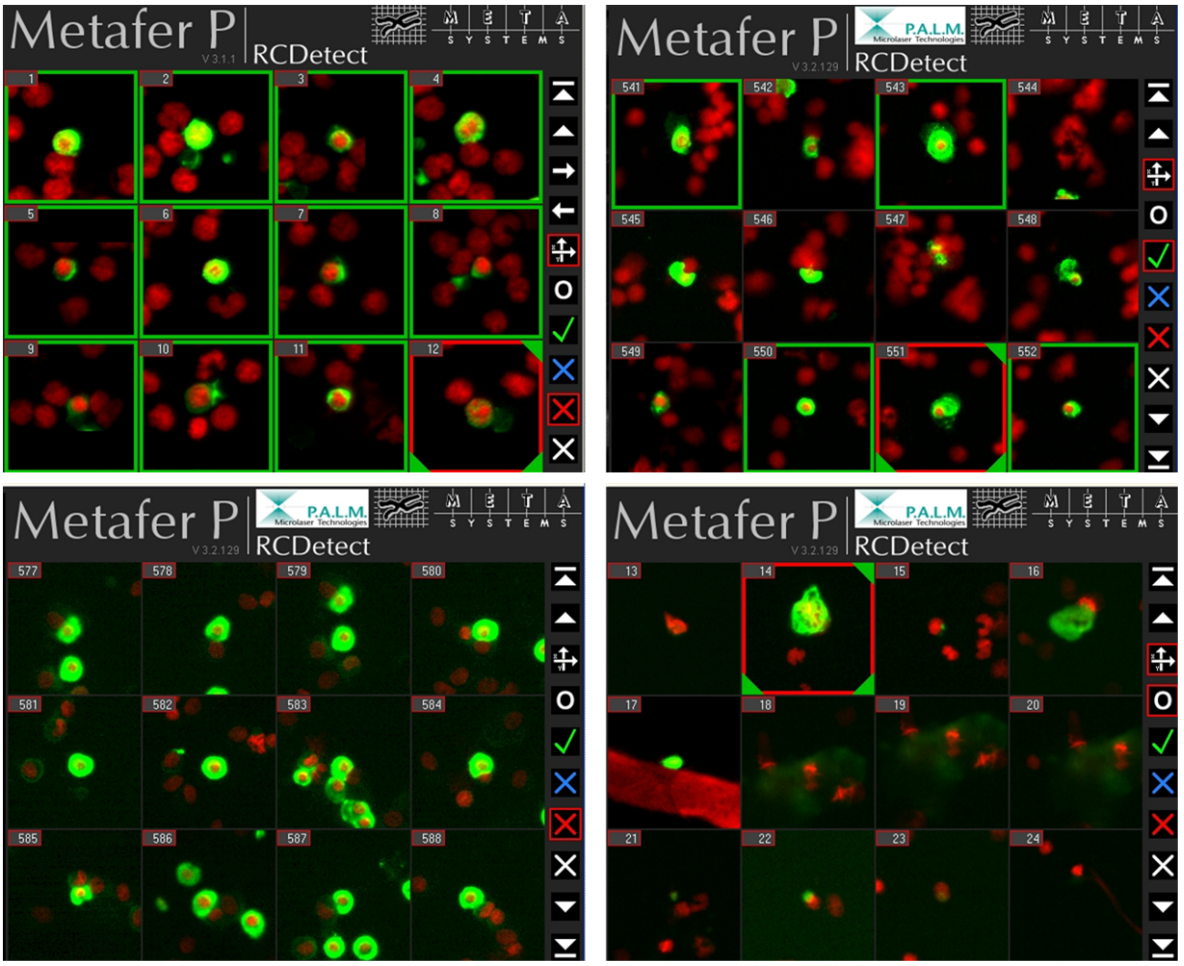

Figure 5: Detection of different cell types
RCDetect was optimized to detect cell types known to circulate in maternal blood such as fetal (top left) and embryonic (top right) erythroblasts and trophoblast cells (bottom left). Furthermore, RCDetect was trained on the detection of large cells such as JAR choriocarcimoma cells (bottom right)

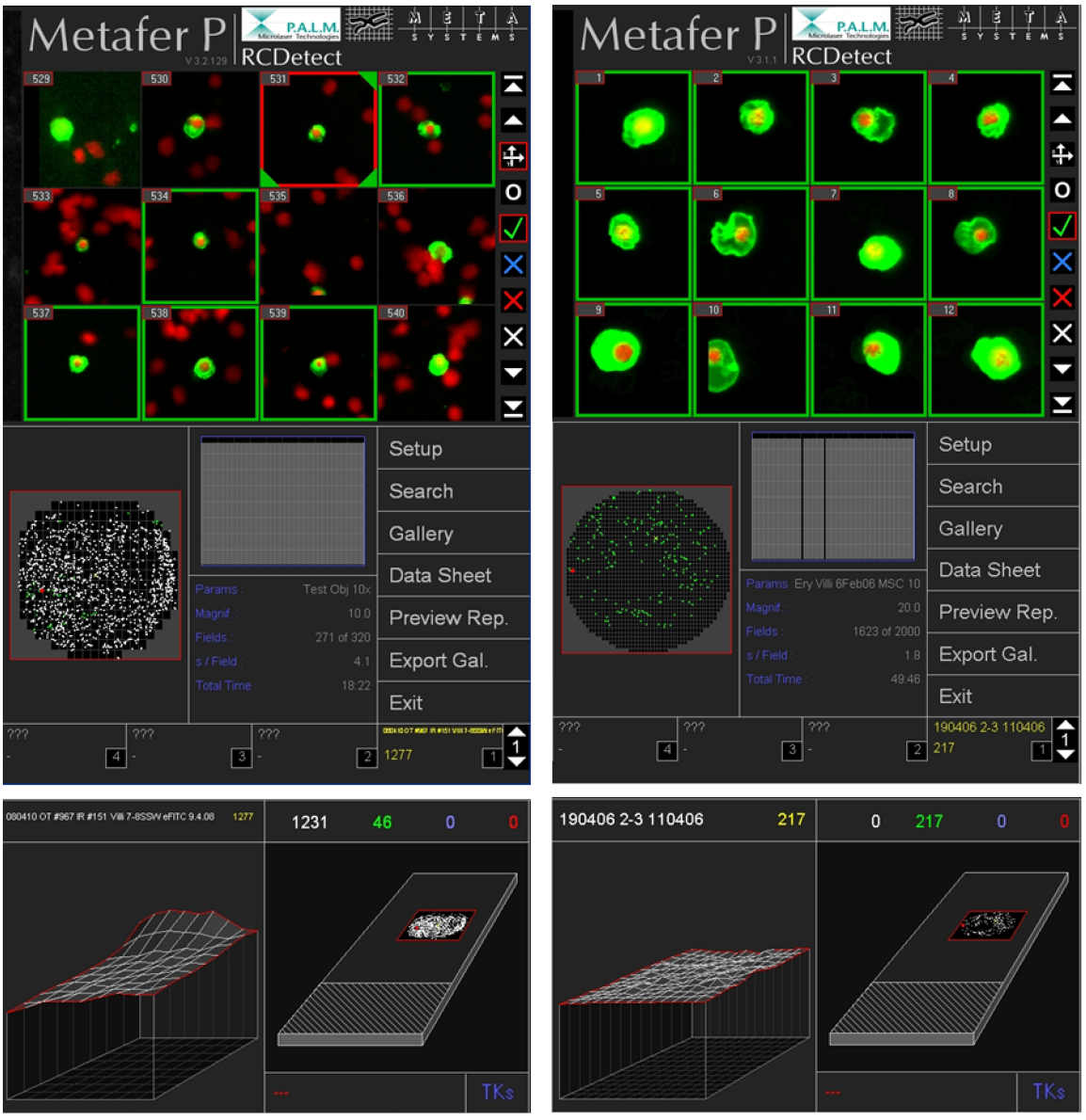

Figure 6: Scanning performance: 10x objective versus 20x objective
User's surface of RCDetect after scanning with 10x (left) and 20x (right) objective clearly showed advantages for the former. Scanning fields were reduced to one-sixth (271 fields vs. 1623 fields). Although scanning time per field increased by factor 2 (4.1 s/field vs. 1.8 s/field; depending on the frequency of filter cube alterations per scan) total scanning time was more than halved (18 min 22 s vs. 49min 46 s).

5.1.3 Using an optimized classifier proved automatic cell detection to be superior to individual screening

The performance of the generated classifier was tested against visual examination of the slides by two lab members familiar with rare cell detection. Therefore, sets of training data containing Hbγ^+ and Hbε^+ erythroblasts were generated containing three different conditions: 1) few scan fields with approx. one target cell (Hbγ^+/TO-PRO-3$^+$ erythroblasts) per field containing a high number of erythrocytes (Hbγ^+/TO-PRO-3$^-$); 2) high number of target cells (Hbε^+/TO-PRO-3$^+$ erythroblasts) per scan field; 3) high number of scan fields containing a very low

total number of target cells (Hbε$^+$/TO-PRO-3$^+$ erythroblasts). For condition 1 the training data of classifier development were used (section 7, Figure 3). For condition 2 Hbε$^+$ erythroblasts were enriched from 1° trimester villous tissue derived from termination of pregnancy. For enrichment chorionic villous tissue was processed according to the enzymatic digest protocol (section 4.5.2). The erythroblast fraction was isolated from the interphase between 6th and 7th density gradient layer and contained a high number of erythroblasts. An aliquot of this erythroblast fraction was then diluted into 25 ml of PBS rinsed PBMNCs from a healthy male donor. From this spiked sample cell enrichment was performed using non-physiological conditions as described in section 7.1.3. Both samples processed from chorionic villous tissue (condition 2 and 3) were cytocentrifuged onto glass slides (section 7.2) and stained using directly labeled anti-Hbγ and anti-Hbε antibodies (section 7.3.2).

Training data and data from slide scanning were retrieved (conditions 1 to 3). The training data were visually checked for positive cells by two lab members and the respective cell counts recorded. The image galleries created by RCDetect from the same slides using the classifier “Ery Villi 6Feb06” (optimized for scanning with 20x objective) were also checked for positive cells and compared to the findings of the visual screening (Table 12).

Table 12: Detection efficiency outcome: RCDetect vs. individual scanning
Different conditions regarding positive cell frequency and signal intensity were tested. When the cells to be detected were rare, automated scanning and counting performed better than visual counting.

Condition	Scan fields [n]	Positive cells detected (RCDetect)	Positive cells detected (visual check)
1	15	14	14
2	122	535	535
3	1867	36	35

5.1.4 Detection of a Hbγ$^+$ cell enriched from peripheral blood of a pregnant woman (12th week of gestation)

I performed enrichment of erythroblasts from peripheral blood of a pregnant woman at 12 weeks of gestation to test the classifier’s applicability under clinical conditions. For density gradient centrifugation, the basic protocol was slightly changed as I used a non-physiological approach following a protocol of Sitar *et al.* (31) as described in section 7.1.3. MACS, cytocentrifugation and direct IF labeling

was performed according to basic protocols (sections 7.1.4, 7.2 and 7.3.2, resp.). As shown in Figure 7, automatic scanning yielded one Hbγ$^+$ erythroblast proving the classifier to be applicable to clinical samples.

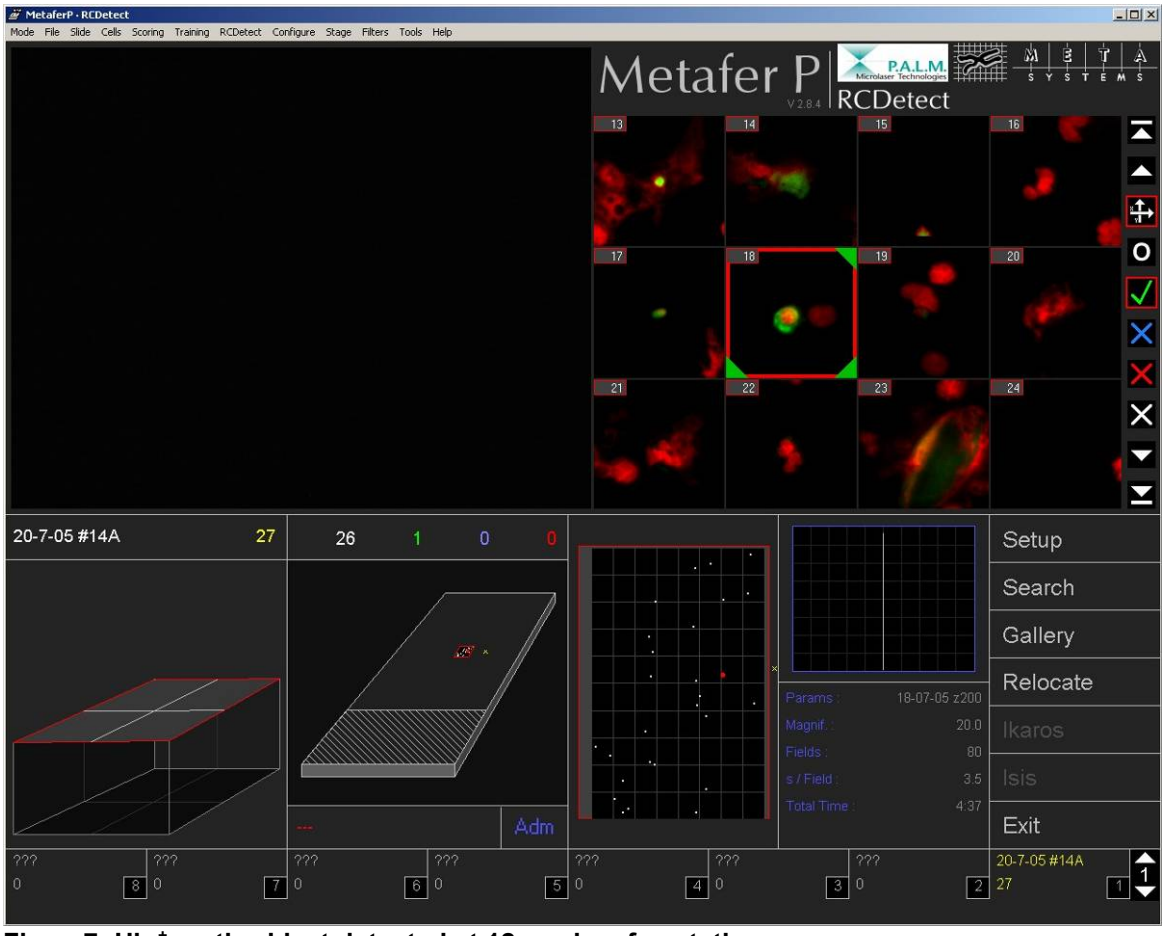

Figure 7: Hbγ$^+$ erythroblast detected at 12 weeks of gestation
7.3ml of peripheral blood of a woman at 12 weeks of gestation were drawn, enriched via MACS (CD71-MicroBeads) and labeled by means of immunofluorescence (anti-Hbγ antibody). After counterstaining (TO-PRO-3) and mounting, the cells were forwarded to automatic scanning using the classifier "18-07-05 z200". Positive events were displayed in the RCDetect image gallery. In this gallery, event number 18 shows (red outlined, green edged box) an Hbγ$^+$ erythroblast located next to an Hbγ$^-$ neutrophil granulocyte. Detection of this erythroblast from peripheral blood proved the classifier, which was developed from cord blood erythroblasts (sampled shortly after delivery) to be feasible for the purpose conceived

5.1.5 Settings of classifier "Test Obj 10x"

The Metafer parameters and focus settings derived from optimizing the classifiers were implemented into classifier "Test Obj 10x". The respective data are given in Figure 8 and Figure 9.

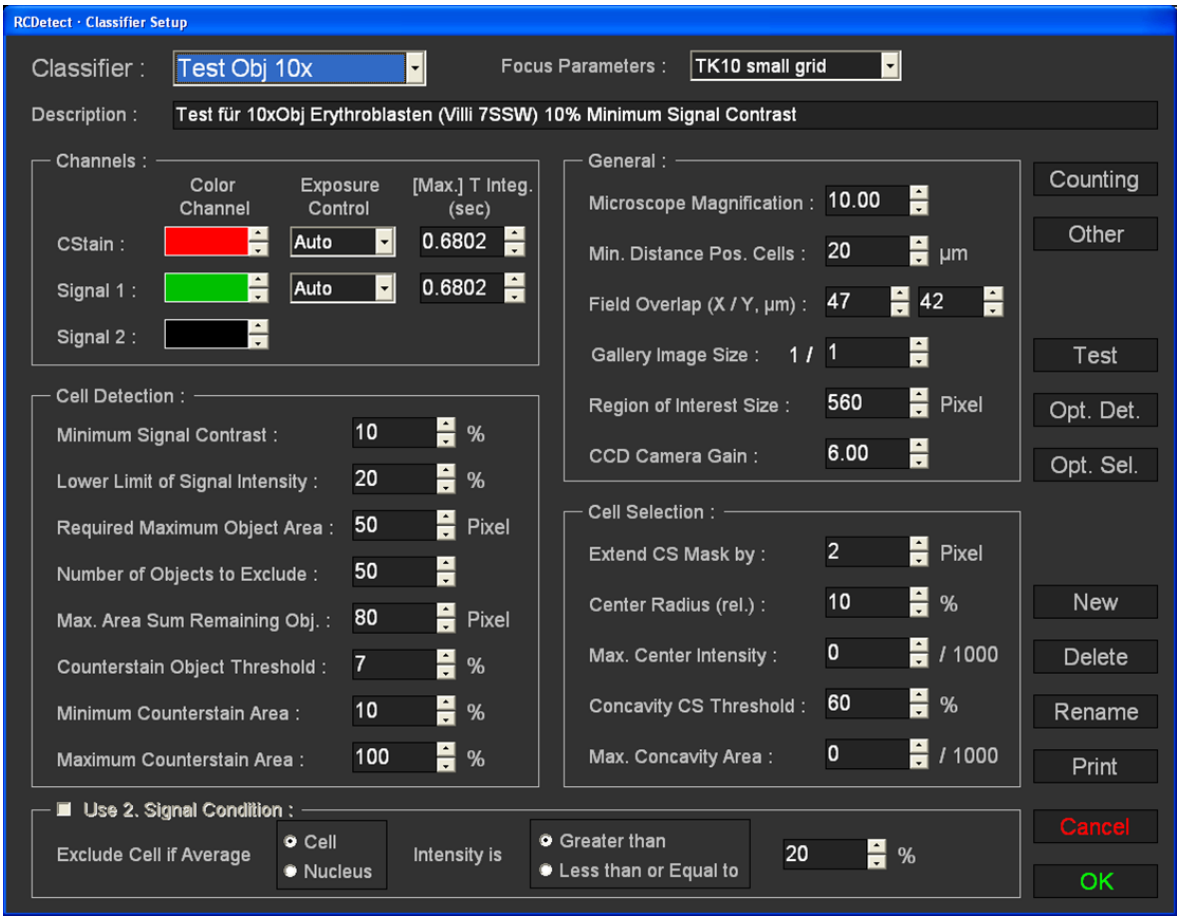

Figure8: Parameter settings of "Test Obj 10x" classifier

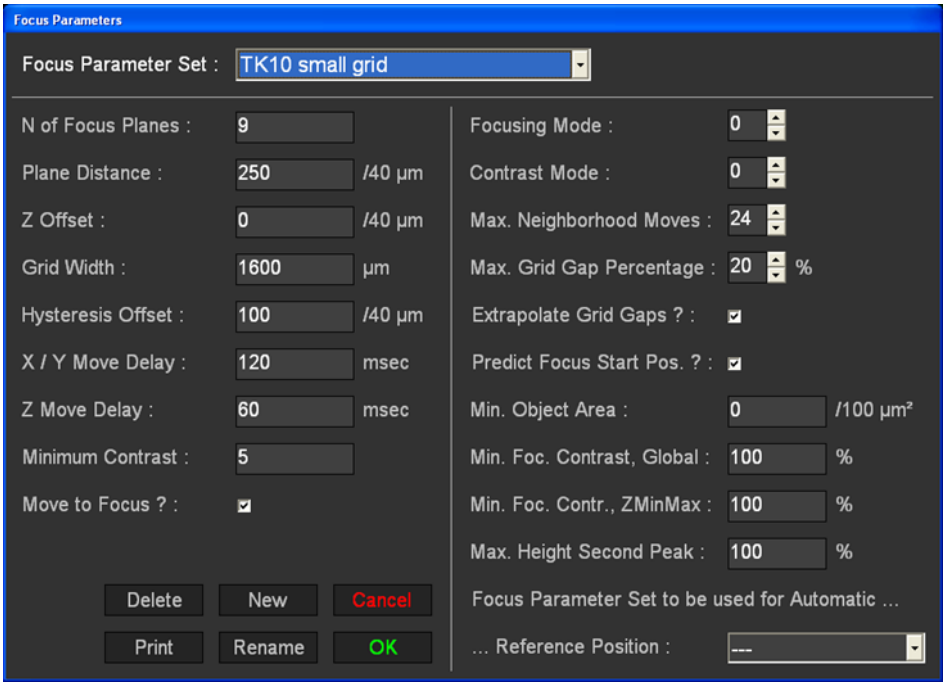

Figure9: Focus parameter settings of "TK10 small grid"
The focus parameter settings of "TK10 small grid" are used with the classifier "Test Obj 10x"

5.2 Development of cell capture setting on AmpliGrid slides

Laser microdissection and pressure catapulting represents the link between the cell enrichment and detection part and the molecular genetic analysis part of this procedure designed to establish a continuous process from sampling to result. Lacking a possibility to correctly position the anchors of the chip for cell collection, I developed a device allowing the alignment of anchors with the respective cells thereby enabling the implementation of this low-volume on-chip amplification method into the process. The main parts are two distance pieces mounted to the lateral ends of the AmpliGrid guaranteeing both enough distance between slide and chip, so that collection droplets do not touch the slide, and minimal flight distance for catapulted cells. This way the score rate has been optimized (Figure 10: PEN membrane slide – chip assembly).

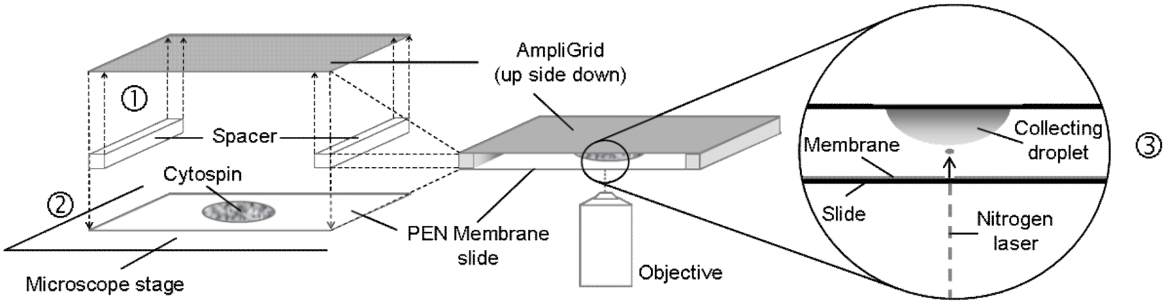

Figure 10: PEN membrane slide – chip assembly
To collect microdissected cells, the anchors of the chip (AmpliGrid) had to be charged with nuclease-free water (collecting droplet) and positioned directly above the candidate cell(s). In order to realize that, I have developed a device enabling the chips' anchors to be positioned above every cell of the cytospin. Therefore, two spacers (height 1 mm) were laterally attached to the chip (1). Upon charging the anchors, this assembly was placed upside down onto the microscope stage (2) and the respective anchor was moved right above the cell(s) for collecting them after LMPC (3).

Using this device the rate of successfully microdissected cells exceeded 95% (175 of 184 catapulting events).

5.3 Performance of rare cell analysis

To assess the feasibility of the method pooled and single cells of all sample types were microdissected and amplified (section 4.8 and 4.9). The PCR products were forwarded to fragment analysis (section 4.11) and the resulting electropherograms were analyzed according to the definitions given in section 4.12.

At first, I generated DNA profiles of each sample type from all of their processed cells (Table 13). Both samples analyzed from PBMNCs sample #1 showed PCR failure. Due to this, a DNA profile could not be assessed and PBMNC sample #1 was excluded from analysis. The same was true for IR #2 in all three pooled cells

samples PCR fragments in 10 of 16 loci (D21S11, D18S51, Penta E, D7S820, D16S539, CSF1PO, Penta D, D8S1179, TPOX, and FGA) were lacking. Thus, IR #2 was excluded from analysis.

Table 13: DNA profiles of sample types
The DNA sample profiles were assessed of all DNA profiles generated from each sample type. Samples containing amplification failure such as PBMNC #1 (no calls at all; not shown) and IR #2 were excluded from further analysis.

Locus	Operator	JAR	PBMNC #2	PBMNC #3	IR #1 (maternal)	IR #1 (fetal)	IR #2 (maternal)	IR #2 (fetal)	IR #3 (maternal)	IR #3 (fetal)
D3S1358	15/16	16/17	15/17	13/15	14/17	14/15	14	14	15/17	15/17
TH01	9.3	6/7	7/9.3	9.3	8/9	8/9.3	7/9	7/8	7/8	7/8
D21S11	31.2/32.2	28/29	29/32.2	28/33.2	28/29	29	-	29/30	30/32.2	30/31.2
D18S51	16/17	14/15	14/16	15/16	13/14	13/15	-	15/16	17	15/17
PentaE	9/17	8/12	8/10	7/22	7/20	7/15	-	7/12	8/12	8/13
D5S818	11	10/11	11/12	12	12/13	13	12/13	12/13	10/12	12/13
D13S317	8/11	11	10/11	11/14	11	11	9/11	9/11	11/12	11/12
D7S820	11	10/11	9/11	10/12	10	10/11	-	8/9	10/12	11/12
D16S539	12/13	9/10	13/14	11/12	10/12	12	-	9/11	9/13	9/12
CSF1PO	11/13	7/10	11/12	12	9/12	9/10	-	12	10/12	8/12
PentaD	12/15	9/14	11/12	10/13	11/13	9/13	-	9/14	9/10	7/9
Amelogenin	XY	XY	X	X	X	X	X	X	X	X
vWA	17	16/18	17/19	17/18	17/18	16/17	17/19	14/19	17	15/17
D8S1179	13/15	14/16	10/15	12/14	14/16	15/16	13	10/14	15/17	14/15
TPOX	8/11	8/11	8	8	9/11	9/11	-	9/11	12	10/12
FGA	21/23	22	22	22/26	19/22	22/22.2	-	22/22.2	22/23	19/23

Homozygous loci are represented by only one allelic repeat such as for the operator's locus TH01; dash: amplification failure, operator: experimenter

5.3.1 PCR efficiency – a parameter for process-related DNA degradation

I calculated the percentage of the detected PCR fragments at heterozygous loci, amplification failure, ADO, and ADI in order to assess the compatibility of the method involving fixation and staining with subsequent PCR. This calculation was made for pooled and single cell samples from two different experimental settings (JAR/PBMNC spikings and interruption tissues, Table 14) as well as for pooled and single cells irrespective of their cell types (Table 15).

In the PBMNC/JAR spiking experiment all PBMNC samples were successfully amplified (100%). ADO occurred in 12.5% (6/48 of heterozygous loci) and amplification failure in 1.6% (1/64 heterozygous and homozygous loci). A heterozygous pattern was detected in 41 of 48 heterozygous loci (85.4%). The PCR efficiency, based on calculation of all PCR fragments detected at heterozygous loci, turned out to be 91.7% (88 of 96 possible PCR fragments). Single JAR cell PCR was successful in 12 of 18 times (66.7%) with an occurrence of ADO in 50 of 168 heterozygous loci (29.8%). Amplification failure was detected in 27.1% of all loci (52/192). A heterozygous pattern was found in 78 of 168 loci (46.4%). PCR efficiency of single JAR cells was determined to be 61.3% (206/336).

PCR from 5 FITC/TO-PRO-3^{+} pooled cells derived from decidual tissues were successful in 10 of 13 cases (76.9%). Of 160 loci 10 failed to amplify (6.3%), ADI was detected in 2 of 160 loci (1.3%), and ADO in 10 of 129 loci (7.8%). A heterozygous pattern was detected in 84.5% (109 of 129 heterozygous loci). Thus, PCR efficiency was calculated to be 88.4% (228 of 258 PCR fragments).

Of 56 single Hbε-positive erythroblasts, trophoblast cells or FITC-negative candidate maternal cells, PCR was successful in 34 cases (76.8%). In these, amplification failure was seen in 190 of 688 loci (27.6%). ADO occurred in 26.9% (150 of 558 loci) and extra alleles (ADI) were detected in 1.5% (10/688). Of 558 heterozygous loci, 252 (45.2%) showed two PCR products, resulting in a PCR efficiency of 58.6% (654/1116).

Table 14: PCR performance in pooled and single cell samples from two different experimental settings

	Female PBMNC of 2 samples		JAR		Cells of 2 interruption tissues			
	Pooled cells (≤10)		Single cells		Pooled cells (5)		Single cells	
	[n / total]	[%]	[n / total]	[%]	[n / total]	[%]	[n / total]	[%]
Successful PCR[1]	4/4	100	12/18	66.7	10/13	76.9	43/56	76.8
# of heterozygous loci[2]	varying		14		varying		varying	
Amplification failure[3]	1/64	1.6	52/192	27.1	10/160	6.3	190/688	27.6
Allele drop-in[4] (all loci)	0/64	0	0/192	0	2/160	1.3	10/688	1.5
Allele drop-out[5] (heterozygous loci)	6/48	12.5	50/168	29.8	10/129	7.8	150/558	26.9
Heterozygous pattern[6] (heterozygous loci)	41/48	85.4	78/168	46.4	109/129	84.5	252/558	45.2
PCR efficiency[7] (heterozygous loci)	**88/96**	**91.7**	**206/336**	**61.3**	**228/258**	**88.4**	**654/1116**	**58.6**

1 PCR yielding at least one amplification product
2 Heterozygous loci of the respective samples as seen from PCR profiles (used for calculating ADO and PCR efficiency)
3 Number and percentage of loci yielding no PCR fragment
4 Extra peaks matching no profile
5 Heterozygous loci yielding only one fragment (heterozygous loci only)
6 Loci showing two allele repeats (heterozygous loci only)
7 Total number of PCR fragments calculated from heterozygous loci

Table 15: PCR efficiency based on the number of cells used as template

	Cell pools (≤10)		Cell pools (5)		Single cells		Over-all	
	[n/total]	[%]	[[n/total]	[%]	[n/total]	[%]	[n/total]	[%]
Successful PCR[1]	4/4	100	10/13	76.9	55/74	74.3	69/91	75.8
amplification failure[2]	1/64	1.6	10/160	6.3	242/880	27.5	253/1104	22.9
allele drop-in[3] (all loci)	0/64	0	2/160	1.3	10/880	1.1	12/1104	1.1
allele drop-out[4] (heterozygous loci)	6/48	12.5	10/129	7.8	200/726	27.5	216/903	23.9
heterozygous pattern[5] (heterozygous loci)	41/48	85.4	109/129	84.5	330/726	45.5	480/903	53.2
PCR efficiency[6] (heterozygous loci)	**88/96**	**91.7**	**228/258**	**88.4**	**860/1 452**	**59.2**	**1176/1806**	**65.1**

1 PCR yielding at least one amplification product
2 Number and percentage of loci yielding no PCR fragment
3 Extra peaks matching no profile
4 Heterozygous loci yielding only one fragment (heterozygous loci only)
5 Loci showing two allele repeats (heterozygous loci only)
6 Total number of PCR fragments calculated from heterozygous loci

5.3.2 Genetic fingerprinting – distinguishing between cells originating from different individuals

The DNA profiles from all samples yielding at least one PCR product were compared to the respective full profiles given in Table 13. The data regarding the JAR and PBMNC samples #2 and #3 are shown in Table 16 and Table 17, the data of the samples from IR #1 and IR #3 can be seen in Table 18 and Table 19, respectively.

Table 16: DNA profiles of JAR cells and PBMNC sample #2

Locus	Profile			Cell pools		Single cells						
	JAR	PBMNC	Operator	B1	B7	B2	B3	B4	B5	B6	B8	B12
D3S1358	16/17	15/17	15/16	15/17	15/17	17	-	17	17	17	17	-
TH01	6/7	7/9.3	9.3	7/9.3	7/9.3	7	-	6	6	-	6/7	-
D21S11	28/29	29/32.2	31.2/32.2	29/32.2	29/32.2	-	-	28	28	-	28/29	-
D18S51	14/15	14/16	16/17	14	14/16	14	-	14	15	-	14/15	-
PentaE	8/12	8/10	9/17	8/10	8/10	8	-	12	8	-	8/12	-
D5S818	10/11	11/12	11	11	11/12	10	-	10	10/11	-	10	-
D13S317	11	10/11	8/11	11	10/11	-	11	-	-	-	11	-
D7S820	10/11	9/11	11	11	9/11	11	-	10	10	10	10/11	-
D16S539	9/10	13/14	12/13	13	13/14	10	-	9/10	9	-	10	9
CSF1PO	7/10	11/12	11/13	-	11/12	-	10	10	-	-	7/10	-
PentaD	9/14	11/12	12/15	11/12	11/12	-	-	9	9/14	9	9	-
Amelogenin	XY	X	XY	X	X	-	X	XY	-	-	Y	X
vWA	16/18	17/19	17	17/19	17/19	16	-	18	18	-	16/18	-
D8S1179	14/16	10/15	13/15	10/15	10/15	-	-	16	16	16	14/16	-
TPOX	8/11	8	8/11	8	8	8/11	-	11	8	11	8/11	-
FGA	22	22	21/23	22	22	-	-	-	-	-	22	-
FITC				-	-	+	+	+	+	+	+	+
Allelic drop-in												
Contamination												
Allocation												

Unambiguous JAR alleles	Unambiguous PBMNC alleles	JAR/PBMNC alleles	(Number)	Allele peak < 100 pts in height but well detectable
Homozygous JAR loci	Homozygous PBMNC loci	Alleles of operator	Number	Allele drop-in/erroneous PCR fragment

Figures represent the numbers of allelic repeats of the marker STR and amelogenin, respectively. For example: Regarding TH01 locus ([AATG] tetranucleotide repeat units) JAR cells should yield two distinct peaks at 164 bp and 168 bp [(66); PCR Product Sizes of observed Alleles, Set 6]. These PCR fragments represent alleles containing a 6-fold and 7-fold [AATG] repeat (residual base pairs result from primer design clamping that STR region) denominated as "6/7". PBMNCs were also heterozygous for that locus yielding 168 bp and 179 bp fragments. The latter PCR fragment represents nine [AATG] repeat units plus one truncated ATG in between repeat number six and seven ($[AATG]_6ATG[AATG]_3$). By nomenclature this allele is designated by the number of complete repeat units (9) and the number of base pairs of the partial repeat (3) separated by a decimal point. Therefore, the correct denomination is 7/9.3. The alleles of pooled and single cells were compared to JAR and PBMNC profiles in order to allocate the respective loci to either JAR (marked in green) or PBMNC (marked in red) origin or to detect contamination (when matching the operator's profile). Loci that yielded allelic repeats matching both profiles (like in TH01 locus of the single cell B2) are indicated in green-red striped. Allocation of cell pools or single cells was considered valid when all loci within one profile consisted of striped and either red or green boxes only (color code in line "allocation"). Column D10: negative control (PCR-clean water), column D12: positive control (100 pg of 9947A Promega control DNA). No amplification of samples B9, B10 and B11 (cell pools) and C4, C8 and C9 (single cells) (not shown).

Table 17: DNA profiles of JAR cells and PBMNC sample #8

Locus	Profile			Cell pools		Single cells					H_2O	9947A
	JAR	PBMNC	Operator	C1	C7	C2	C3	C10	C11	C12	D10	D12
D3S1358	16/17	13/15	15/16	13/15	13/15	16/17	16/17	16/17	16/17	16/17	-	14/15
TH01	6/7	9.3	9.3	9.3	9.3	6/7	6/7	6/7	6/7	6/7	-	8/9.3
D21S11	28/29	28/33.2	31.2/32.2	28/33.2	28/33.2	28/29	29	28	28/29	28/29	-	30
D18S51	14/15	15/16	16/17	15/16	15/16	14/15	14	14/15	14/15	14/15	-	15/19
PentaE	8/12	7/22	9/17	7/22	7/22	12	8/12	8/12	8/12	8/12	-	12/13
D5S818	10/11	12	11	12	12	10/11	10/11	10/11	10/11	10/11	-	11
D13S317	11/11	11/14	8/11	11/14	11/14	11	11	11	11	11	-	11
D7S820	10/11	10/12	11	10/12	10/12	10/11	10/11	10/11	10/11	10/11	-	10/11
D16S539	9/10	11/12	12/13	11/12	11/12	9/10	9/10	9/10	9/10	9/10	-	11/12
CSF1PO	7/10	12	11/13	12	12	7/10	7/10	7/10	7/10	7/10	-	10/12
PentaD	9/14	10/13	12/15	10/13	10/13	9/14	9/14	9/14	9/14	9/14	-	12
Amelogenin	XY	X	XY	X	X	XY	XY	-	XY	XY	-	X
vWA	16/18	17/18	17	17/18	17/18	16/18	16/18	16/18	16/18	16/18	-	17/18
D8S1179	14/16	12/14	13/15	12/14	12/14	14/16	14/16	14/16	14/16	14/16	-	13
TPOX	8/11	8	8/11	8	8	8/11	11	8/11	8/11	8/11	-	8
FGA	22/22	22/26	21/23	22/26	22	22	22	22	22	22	-	23/24
FITC				-	-	+	+	+	+	+		
Allelic drop-in												
Contamination												
Allocation												

For color code see the legend in Table 16

Table 18: DNA profiles of fetal and maternal cells obtained from tissue from termination of pregnancy (IR #1)

Locus	Profile			Cell pools				Single cells				
	Fetal	Maternal	Operator	B1	B6	D6	D12	B2	B3	B5	B7	B8
D3S1358	14/15	14/17	15/16	14/15	14/15	14/17	14/17	14	14/15	-	14/15	14/15
TH01	8/9.3	8/9	9.3	8/9.3	8	8/9	-	-	8	-	-	-
D21S11	29	28/29	31.2/32.2	29	29	28/29	29	-	29	-	29	(29)
D18S51	13/15	13/14	16/17	13/15	13/15	13/14	-	-	-	-	15	-
PentaE	7/15	7/20	9/17	7/15	7/15	7/15/20	-	-	7	-	-	(7)
D5S818	13	12/13	11	13	13	12/13	12/13	13	-	13	13	-
D13S317	11	11	8/11	11	11	11	11	-	11	-	11	-
D7S820	10/11	10	11	10/11	10/11	10	10	-	10/11	-	10	(11)
D16S539	12	10/12	12/13	12	12	10/12	-	-	12	-	12	12
CSF1PO	9/10	9/12	11/13	9/10	9/10	9/12	-	-	9/10	-	(9)/10	9/10
PentaD	9/13	11/13	12/15	9/13	9/13	11/13	-	-	9	-	-	9/13
Amelogenin	X	X	XY	X	X	X	X	-	X	-	-	-
vWA	16/17	17/18	17	17	17	16/17/18	17/18	17	17	17	17	17
D8S1179	15/16	14/16	13/15	15/16	15/16	14/15/16	14	-	-	-	15/16	-
TPOX	9/11	9/11	8/11	9/11	9/11	9/11	-	-	9/11	-	9	-
FGA	22/22.2	19/22	21/23	22/22.2	22/22.2	19/22	-	-	22.2	-	22	22/22.2
FITC				+	+	-	-	+	+	+	+	+
Allelic drop-in												
Contamination						+						
Allocation												

Table 18 continued

Locus	Single cells												H_2O
	B9	B10	B11	C2	C4	C5	C6	C7	D3	D4	D7	D8	C12
D3S1358	14/15	14	-	-	15	14/15	-	14/15	-	-	15	-	-
TH01	8	-	-	-	9.3	-	-	8	-	-	-	-	-
D21S11	29	29	-	-	-	29	-	29	29	29	29	-	-
D18S51	13	15	-	-	13/15	13/15	-	13/15	-	-	-	-	-
PentaE	-	-	-	-	7	7	-	7/15	-	-	20	-	-
D5S818	-	13	-	-	13	13	-	13	-	-	-	-	-
D13S317	11	11	11	-	11	11	-	11	-	-	11	11	-
D7S820	11	10/11	-	-	10	10/11	-	10/11	10	-	-	-	-
D16S539	12	12	-	-	12	12	-	12	-	-	10/12	-	-
CSF1PO	9/10	-	-	-	9	9/10	-	9/10	9	12	-	9	-
PentaD	9/13	-	-	-	13	9/13	-	9/13	-	-	11	-	-
Amelogenin	X	-	-	-	-	-	-	X	X	X	X	X	-
vWA	17	17	17	15	17	17	17	17	17/18	18	-	-	-
D8S1179	-	16	-	-	15	15/16	-	15/16	14	-	-	-	-
TPOX	11	-	-	-	9	9/11	-	-	-	-	-	-	-
FGA	22/22.2	22	-	-	22	22	-	22/22.2	-	19/22	19/22	22	-
FITC	+	+	+	+	+	+	+	+	-	-	-	-	
Allelic drop-in				+							+		
Contamination													
Allocation													

Figures represent the allelic repeats of the STR markers and amelogenin, respectively. Loci displaying the maternal allelic patterns are marked in red; loci matching the allelic patterns of fetal cells are indicated in green. Loci showing allele repeats matching both profiles (fetal/maternal cells) are indicated in green-red striped. Red numbers are used to highlight extra peaks (ADI) matching none of the profiles. Controls are as described in the legend to Table 16. No amplification at B12 and D1 (cell pools) and at B4, C1, C3, D2, D5 and D8 (single cells). The profile of the operator is given to provide information concerning contamination.

Table 19: DNA profiles of fetal and maternal cells obtained from interruption material (IR #3)

Locus	Profile			Cell pools					
	Fetal	Faternal	Operator	A7	B7	C1	D7	D8	D9
D3S1358	15/17	15/17	15/16	15/17	15/17	15/17	15/17	15/17	15/17
TH01	7/8	7/8	9.3	7/(8)	7/8	7/8	7/8	7/8	7/8
D21S11	30/31.2	30/32.2	31.2/32.2	30/31.2	30/31.2	30/31.2/32.2	30/32.2	30/32.2	30/32.2
D18S51	15/17	17/17	16/17	15/17	15/17	15/17	17	17	17
PentaE	8/13	8/12	9/17	8/13	8/13	8/12/13	8/12	-	-
D5S818	12/13	10/12	11	12/13	12/13	10/12/13	10/12	10/12	10/12
D13S317	11/12	11/12	8/11	12	12	(11)/12	11/12	11/12	11/12
D7S820	11/12	10/12	11	11/12	11/12	10/11/12	10/12	10/12	10/12
D16S539	9/12	9/13	12/13	9/12	9/12	9/12/13	9/13	9/13	9/13
CSF1PO	8/12	10/12	11/13	8/12	8/12	8/12	12	12	10
PentaD	7/9	9/10	12/15	7/9	7/9	7/9/10	9/10	9/10	9/10
Amelogenin	X	X	XY	X	X	X	X	X	X
vWA	15/17	17	17	15/17	15/ 16/17	15/17	17	17	17
D8S1179	14/15	15/17	13/15	14/15	14/15	14/15/17	15/17	15/17	15/17
TPOX	10/12	12	8/11	10/ 11/12	10/12	10/12	12	12	12
FGA	19/23	22/23	21/23	19/23	19/23	19/22/23	22/23	22/23	22/23
FITC				+	+	+	-	-	-
Allele drop-in				+	+				
Contamination						+			
Allocation									

The figures represent the allelic repeats of STR markers and amelogenin. For color code see the legend in Table 16. No amplification at A1 (cell pools) and at A4, A10, B1, B5, B10, B11 and C6 (single cells). The profile of the operator is given for the purpose of detecting contaminations.

Table 19 continued

Locus	Single cells (Hb)								
	A2	A3	A5	A6	A8	A9	A11	A12	B2
D3S1358	15/17	15/17	15/17	15/17	15/17	(15)	15/17	(15)/17	15/17
TH01	7	7/8	8	8	7	8	-	-	8
D21S11	30/31.2	30/31.2	30/31.2	30	30/31.2	30/31.2	30/31.2	30/31.2	30/31.2
D18S51	(13)/15/17	15/17	15/17	15/17	-	(15/17)	(17)	15/(17)	15/17
PentaE	8/13	8/13	8/13	13	-	-	-	-	(8)/13
D5S818	12/13	12/13	12/13	12/13	12/13	(12/13)	12/13	12/13	12/13
D13S317	11/12	12	11/12	12	12	12	12	12	12
D7S820	11/12	11/12	11/12	11	11/12	11/12	11/12	11	11/12
D16S539	9/12	9/12	9/12	9	9/12	9/12	9	9/12	9/12
CSF1PO	8/12	8/12	8/12	8/12	8/12	8/12	-	-	12
PentaD	7/9	7/9	7/9	7/9	7/9	-	7/9	7/9	7/9
Amelogenin	X	X	X	X	X	(X)	X	X	X
vWA	15/17	15/17	15	17	15/17	15	15/17	15/17	15/17
D8S1179	14/15	13/14/15	14/15	15	15	-	-	-	14/15
TPOX	8/10/12	10/12	10/12	-	12	12	-	-	10/12
FGA	19/23	19/23	19/23	-	19/23	23	19/23	23	19
FITC	+	+	+	+	+	+	+	+	+
Allele drop-in	+	+							
Contamination									
Allocation									

Table 19 continued

Locus	Profile			Single cells (GZ158/GZ112)					
	Fetal	Maternal	Operator	B8	B9	C5	C8	C9	C10
D3S1358	15/17	15/17	15/16	15/17	15/17	15/17	15/17	15	15/17
TH01	7/8	7/8	9.3	7	7/8	7/8	8	7/8	7/8
D21S11	30/31.2	30/32.2	31.2/32.2	31.2	30/31.2	30/31.2	30/31.2	30/31.2	30/31.2
D18S51	15/17	17	16/17	15/17	15/17	15/17	(14)/15	15/17	15/17
PentaE	8/13	8/12	9/17	8	8/13	8/13	8/13	-	-
D5S818	12/13	10/12	11	12/13	12/13	12/13	12/13	11/12/13	12/13
D13S317	11/12	11/12	8/11	12	12	12	12	12	12
D7S820	11/12	10/12	11	12	11/12	11/12	11/12	11/12	11/12
D16S539	9/12	9/13	12/13	9	9/12	9/12	9	12	9/12
CSF1PO	8/12	10/12	11/13	12	8/12	8/12	8/(12)	12	12
PentaD	7/9	9/10	12/15	7/9	7/9	7/9	9/7	7/9	7/9
Amelogenin	X	X	XY	X	X	X	X	(X)	X
vWA	15/17	17	17	15/17	15/17	15/17	15/ 16/17	15/17	15/17
D8S1179	14/15	15/17	13/15	14	14/15	-	14	-	14
TPOX	10/12	12	8/11	12	10/(12)	10/12	10/12	12	(10)/12
FGA	19/23	22/23	21/23	19/23	19/23	19/23	19/23	19/23	19/23
FITC				+	+	+	+	+	+
Allele drop-in							+	+	
Contamination									
Allocation									

For color code see the legend in Table 16.

Table 19 continued

Locus	Single cells negative for Hb and GZ158/GZ112								
	B12	C2	C3	C4	C7	C11	C12	D3	D4
D3S1358	15/17	17	15/17	15/17	15	17	(15)	15/17	15
TH01	-	7	7/8	7/8	8	-	-	8	7
D21S11	30/32.2	30/32.2	30/32.2	30/32.2	30/31.2/(32.2)	30/32.2	30	30/32.2	32.2
D18S51	17	17	15	17	17	17	-	17	17
PentaE	-	-	8/12	8/12	8/12	-	-	8/12	12
D5S818	10/12	10/12	10/12	10/12	-	10	(10/12)	10/12	-
D13S317	11/12	11/12	11/12	11/12	-	11/12	11/12	11/12	11/12
D7S820	10/12	10	12	10/12	12	10/12	10/12	10/12	(10)/12
D16S539	9/13	13	13	9/13	9/13	8/9/13	(9/13)	9/13	13
CSF1PO	-	12	12	12	12	-	-	12	-
PentaD	(9)/10	-	10	10	9/10	9/10	-	10	9/10
Amelogenin	X	X	X	X	X	X	-	X	-
vWA	17	17	17	17	17	17	17	17	17
D8S1179	15/17	15/17	15/17	15/17	-	-	-	15/17	-
TPOX	-	12	-	12	12	-	-	12	12
FGA	22/23	22	23	22/23	22/23	22/23	22	22	22/23
FITC	-	-	-	-	-	-	-	-	-
Allele drop-in			+		+	+			
Contamination									
Allocation									

Table 19 continued

Locus	Profile			Single cells (Hoechst)		H_2O	9947A
	Fetal	Maternal	Operator	B3	B6	D10	D12
D3S1358	15/17	15/17	15/16	15/17	(14)/15/17	-	14/15
TH01	7/8	7/8	9.3	7/8	7/8	-	4
D21S11	30/31.2	30/32.2	31.2/32.2	30/31.2	30/31.2	-	30
D18S51	15/17	17	16/17	15	15	-	15/19
PentaE	8/13	8/12	9/17	-	8	-	-
D5S818	12/13	10/12	11	12/13	12/13	-	11
D13S317	11/12	11/12	8/11	12	12	-	11
D7S820	11/12	10/12	11	11/12	12	-	10/11
D16S539	9/12	9/13	12/13	9	9/12	-	11/12
CSF1PO	8/12	10/12	11/13	8/12	-	-	14/15
PentaD	7/9	9/10	12/15	9	7/(9)	-	12
Amelogenin	X	X	XY	X	X	-	X
vWA	15/17	17	17	15/17	15/17	-	16/17/18
D8S1179	14/15	15/17	13/15	15	14/15	-	13
TPOX	10/12	12	8/11	10/12	10/12	-	8
FGA	19/23	22/23	21/23	23	19/22/23	-	23/24
FITC				+	+		
Allele drop-in					+		
Contamination							
Allocation							

For color code see the legend in Table 16.

All 16 analyzed samples from JAR/PBMNC spikings could be allocated to either JAR or PBMNC origin due to their unambiguous PCR profiles (Table 16). The negative and positive control confirmed absence of contamination and correct PCR setting, respectively.

Regarding the data from IR #1, 21 DNA profiles were retrieved and analyzed (Table 18). Among these samples, four cell pools were processed. Two of which contained FITC$^+$/TOPRO-3$^+$ the other two FITC/TOPRO-3$^+$ cells. Both FITC$^+$ cell pools unambiguously matched the fetal profile. One of the two FITC$^-$ cell pools could be allocated to the maternal profile, whereas the second showed triallelic pattern in 3 of 13 informative loci (Penta E, vWA and D8S1179). Another four loci did not exclude fetal contamination since in these loci the sample yielded a heterozygous pattern whereas the fetal pattern was homozygous (D21S11, D5S818, D16S539) or the data were uninformative (D7S820). The sample therefore was recognized as maternal sample contaminated with FITC$^+$ fetal cells. Furthermore, I analyzed 17 single cells. Of 13 FITC$^+$ single cells, eight matched the fetal profile. Further four FITC$^+$ cells could not be allocated to one of the DNA profiles because all detected allele repeats turned out to be uninformative. Sample C2 (FITC$^+$ single cell) displayed a single PCR drop-in fragment. Out of four FITC$^-$ negative, presumably maternal cells, DNA profiling confirmed the presence of a

maternal genome in two cases; a further one showed unambiguous loci for both profiles (one fetal, four maternal, three inconclusive). In this case, it is very likely that allele drop-in occurred in one locus (D3S1358) mimicking fetal identity. The 4th cell yielded inconclusive results.

From IR #3 a total of 32 samples was analyzed (Table 19), six of which were pooled samples containing either five Hbε+/TO-PRO-3+ cells (A7, B7 and C1) or FITC/TO-PRO-3+ cells (D7, D8 and D9). All three FITC pooled cell samples yielded maternal DNA profile. Two Hbε+ pooled erythroblast samples were confirmed to be of fetal origin due to DNA profiling; ADI was detected in both cases. The third pooled sample was contaminated as eight loci turned out to be triallelic displaying both maternal and fetal alleles.

I further analyzed eleven single Hbε+/TO-PRO-3+ erythroblasts, six single (GZ158 / 112)+/TO-PRO-3+ trophoblast cells and another nine single TO-PRO-3+ cells negative for Hbε, GZ158 and GZ112. The DNA profiles confirmed fetal origin of all 17 FITC+ erythroblasts and trophoblast cells, respectively. ADI was detected in three erythroblasts (A2, A3 and B6) and two trophoblast cells (C8 and C9); fitting the operators profile in three cases (A2, A3 and C9). The DNA profiles of the nine FITC samples could be allocated to maternal origin, although ADI was detected in three samples (C3, C7 and C11) mimicking fetal specific alleles in two cases (C3 and C7). Since these were single cells, it is likely that ADI mimicking fetal pattern occurred. There were no profiles showing only inconclusive loci.

Unambiguous allocation to genomic identity was possible in 100% of the cells analyzed from non-related individuals (JAR/PBMNC). Regarding the samples analyzed from related individuals (interruption tissues), 86% could be allocated to their origin. I furthermore identified two contaminated samples (IR #1 D6 and IR #3 C1) and one sample showing a single ADI (IR #1 C2).

6 Discussion

The aim of this work was to develop a method allowing sex- and cell type-independent identification of rare microchimeric cells. Especially non-invasive prenatal diagnosis based upon fetal cells present in the maternal circulation at low frequencies would benefit from that method as current protocols lack a holistic approach.

I therefore designed a method linking cell detection based on automatic screening of cells labeled by immunofluorescence with laser-catapulting of candidate target cells to reaction sites of slides designed for low-volume on-chip PCR. The concept of this method is to define a group of candidate cells using biochemical markers that need not be perfectly specific but of relevant sensitivity for the detection of target cells. The candidate cells are forwarded to DNA fingerprinting analysis and the resulting DNA profiles are then used for allocating the analyzed cells to the respective individuals.

6.1 Automated detection

The classifier I have developed is able to detect a variety of different cell types such as fetal ($Hb\gamma^+$, Figure 3, Figure 5 and Figure 7) and embryonic ($Hb\varepsilon^+$, Figure 5 and Figure 6) erythroblasts, trophoblast cells (Figure 5), and JAR choriocarcinoma cells (Figure 5), all of which are likely to represent rare circulating cells. In addition, detection of other cell types such as adenocarcinoma cells (HT-29) or melanoma cells (SK-MEL-30) analyzed from cell spiking is possible, too (data not shown). Due to this classifier's high tolerance regarding the detected staining pattern it is able to detect surface stainings as well as cytoplasmatic stainings. Thus, it may be used to detect known epitopes and is applicable to future markers.

The automated scanning software RCDetect used in this method proved to be accurate as it scored a detection rate of 100% in three different settings. These settings were designed to test correct cell counting under the conditions (a) "high erythrocyte background", (b) "short target cell interspace" and (c) "few target cells" (Table 12). Individual and automated scanning yielded no differences in the first two settings. However, when cell counting was performed under "few target cells" conditions the individual scanning failed to detect one target cell proving

automated scanning to be the more accurate method. In addition to its higher reliability, automated scanning relieves lab personnel from cumbersome visual screening of slides.

I have developed this classifier using model systems such as cord blood erythroblasts or erythroblasts derived from tissues after termination of pregnancies. To prove the classifier's applicability to clinical samples I processed peripheral blood of a woman at 12 weeks of gestation (5.1.4). The enriched and stained cell fraction was forwarded to automated cell detection using RCDetect software. The scanning yielded one $Hb\beta^{+}$ erythroblast, proving this way the cell detection in clinical samples for feasibility.

6.2 Performance of rare cell analysis

Regarding the use of fixed and labeled cells with single cell DNA fingerprinting two main questions had to be answered: Is the method consisting of fixation, labeling and laser microdissection compatible to single cell DNA fingerprinting? And secondly, allows DNA fingerprinting to distinguish between cells sharing a haploid set of chromosomes?

6.2.1 Fixation, labeling scanning and laser microdissection is compatible with single cell DNA fingerprinting

DNA fingerprinting performed in a volume of less than 2 µl is shown to be compatible with the preceding processing of cells for pre-identification (establishment of candidate status), making use of DNA profiles as powerful sex-independent markers in single cell analysis.

The multiplex PCR used to identify candidate cells might be combined with an analysis of specific monogenetic genomic disease markers. Working in preparation for implementing whole genome amplification (WGA) of single cells so that aliquots of the expanded genome may be used for identification on the basis of multiplex PCR, and the rest of the WGA of confirmed fetal cells pooled and used for molecular genetic analysis of e. g. monogenetic diseases or chromosome aberrations by array comparative genomic hybridization (CGH).

In previous work, multiplex PCR of STR markers and amelogenin was used with low-volume on-chip PCR, demonstrating its feasibility on minute amounts of DNA. Full DNA profiles were achieved from as little as 32 pg of DNA (67). Analysis of single cells without extraction was recently shown by

Hagen-Mann *et al.* (68). So far, however, it has not been known how fixed, labeled and lysed single cells would perform. In my approach, it has not only been necessary to adapt various steps in the procedure such as cell detection and relocation but also to optimize single cell harvesting. I kept potentially harmful protocol steps such as fixation to a minimum, and adjusted volumes to meet low-volume PCR compatibility. That down-scaling of PCR volumes reduced the cost of reagents and made it possible to control quality visually by seeing whether laser microdissected cells in fact landed on the chip anchor.

My PCR performance data are slightly better than low-volume on-chip PCR performance data reported by Schmidt *et al.* (67), who used dilution series of genomic DNA. They reported PCR failure in 9.1%, 42.7% and 50.0% of DNA template amounts of 63 pg, 32 pg and 8 pg, respectively whereas I had no PCR failure using 10 pooled cells (corresponding to 60 pg of DNA) and no PCR products in 23.1% and 25.7% at the 5-cell and single cell level, respectively. Although it seems that fixed and labeled microdissected cells perform better than purified genomic DNA, it must be taken into account that dilution series contain calculated means of very low amounts of DNA with an unknown deviation. Thus, dilution series down to a few genome equivalents reflect neither calculated quantity nor equally distributed DNA, which may account for the difference. I observed quite a high range of PCR performance between our samples and could identify various factors that may had caused amplification failure specifically in relation to the on-chip approach. Occasionally, during microdissection, dust particles were attracted to the AmpliGrids, causing small air reservoirs to be trapped during subsequent charging of anchors (not shown). That entrapment resulted in extensive evaporation at the aqueous/gaseous interphase underneath the sealing solution and led to an impairment of the PCR assembly. Minor changes in the workflow of laser microdissection and laser pressure catapulting resulted in reduced exposure to air, causing less difficulty for the PCR assembly. However, in some cases, PCR failure could not be traced back to either cause and remained unexplained.

ADO occurred in pooled samples often cells in 12.5% of the cases studied. Although Schmidt *et al*. (67) detected no signs of ADO using 63 pg of genomic DNA (corresponding to 10 cells), they found a higher incidence of ADO at 32 pg

(28.6%) and 8 pg (100%) than when we analyzed pools of five cells (7.8%) and single cells (27.5%). ADO may be due to both cell quality and processing. In DNA profiles of unfixed cells stored at 4°C for approximately one week, I noticed a lower PCR efficiency (obviously due to DNA degradation) in comparison to cells fixed on the second day post sampling (data not shown). Thus, the time between sample collection or cell culture and fixation needs to be kept to a minimum especially for analysis of single cells. Further factors accounting for ADO may include steric blocking of DNA polymerase to DNA due to inefficient cell lysis, strong DNA-histone interaction, or DNA sticking to the hydrophilic surface of the chip anchor.

ADI was detected in 12 of 1104 (1.1%) analyzed loci and maximally occurred once per multiplex PCR. In my work, more than ¾ of the artifacts occurred in a single tissue sample from a pregnancy termination. One positive control, amplified together with the cells from the respective sample, also showed ADI in three loci (TH01, CSF1PO and vWA) indicating that carry-over has taken place during pipetting. Fixation and staining procedures may also increase the frequency of ADI. Although ADI was not reported to occur with diluted genomic DNA, Dietmaier *et al.* observed nonspecific PCR fragments in PCR from a few unfixed but also from pooled fixed cells(69). However, in my hands ADI did not interfere with allocation of cells to their respective origins. Although some of the PCR products matched individual PCR profiles (Table 19: A2, A3, B6, C9), contamination was largely ruled out as PCR was done on single cells. Even when ADI occurred in pooled cell samples (Table 19: A7, B7), it was easily distinguished from contaminated samples (Table 18: D6 and Table 19: C1) due to differences in the number of triallelic STR patterns (one versus three and eight triallelic pattern, respectively). Three samples (Table 18: D7 and Table 19: C3, C7) yielded DNA profiles inconsistent at one locus each. In these cells, specific fetal alleles were detected at loci D3S1358, D21S11 and D18S51, respectively, whereas the residual loci were either uninformative or of maternal origin. Although DNA profiles showed fetal alleles, maternal alleles were four to six times more frequent. I could exclude contamination by fetal cells or cells of the operator because I used single cells and alleles accounting for ADI differed from those of the operator.

6.2.2 Single cell DNA profiles enable to distinguish between cells sharing a haploid set of chromosomes

Cell allocation could be successful on the basis of even a single informative locus (Table 16: B3, B12) but could also fail based on up to four loci (Table 18: D8). Uninformative PCR accounted for up to 70% of the DNA profile (10 of 14 loci; Table 18: C4). These data reflect the difference between both experimental settings used. It is easier to distinguish between cells at low levels of successful amplification when the cells are derived from two non-related individuals. Allocation was successful in more than 88% of cells with 16-plex PCR.

Many approaches described in the literature have used histochemical staining methods that convey little specificity for detection of fetal cells (22, 26, 30, 70-73). PCR performance after histochemical stainings such as May-Grünewald Giemsa, hematoxylin or Wright staining are reported to result in amplification failure from 10% to 58% in cases where erythroblasts were analyzed (22, 26, 70, 72). ADO or contamination occurred in 25% to 62%, uninformative loci were observed in 12.5% to 62.5% in cases where STR markers were used (26, 72). Apart from a few samples, the high number of uninformative cases of the latter resulted from a low number of STR markers used for identification purposes (26). I assume that 16-plex PCR increases the rate of successful confirmation of fetal candidate cells due to a higher number of analyzed loci.

This may even be more crucial to approaches using FISH in rare cell diagnosis. Kolvraa *et al.* could identify false positive XY cells using reverse-color XY-FISH indicating that FISH is error-prone especially when applied in rare cell diagnosis (33). A serious handicap to using Y-FISH is that it is unable to detect female fetal cells. However, probes to detect trisomies (chromosomes 13, 18 and 21) might be used for the discovery of trisomic (fetal) cells. When examining cells derived from normal pregnancies, I observed split FISH signals and nuclei showing trisomic FISH pattern (data not shown). Preliminary data indicate that processing of nuclei for FISH does not interfere with subsequent DNA profiling (not shown), thus allowing for combinatory use to improve single cell analysis.

Enrichment for trophoblast cells is promising using the ISET technique ("isolation by size of epithelial tumor cells") or MACS combined with subsequent short-term culture (18, 30). Both methods try to overcome fetal cell shortage based on conventional enrichment methods. I presume that a combination of one of these

methods with whole genome amplification and DNA fingerprinting is a promising avenue for cell-based NIPD.

I have shown that DNA profiling of single candidate cells under rare cell conditions allows for verification or falsification of their genetic origins in the majority of cases. When rare cells were compared to host cells from unrelated persons, the power of assignment amounted to 100%. I assume that this method will also be helpful to recognize fetal cells of an ongoing pregnancy but also of circulatory cells from previous pregnancies provided the DNA is available (from living children or aborted fetuses). Beyond NIPD, applications may include the analysis of microchimerism in tissues including analysis of the effect of stem cell therapy.

7 Appendix – Basic Protocols

7.1 Basic enrichment protocols

7.1.1 Buffers and solutions

PBS (10 mM), PBS/EDTA and MACS buffer were prepared from 10x stock solutions by dilution with water (ddH_2O or Milli-Q water). The buffers were adjusted to pH 7.3 to pH 7.4.

Table 20: 10x stock solutions of PBS (500mM)

Reagent	[g]
Di-sodium phosphate dodecahydrate ($Na_2HPO_4 \cdot 12\,H_2O$)	29.01
Potassium dihydrogen phosphate (KH_2PO_4)	2.59
Sodium chloride (NaCl)	90.06
ddH_2O	ad 1000 ml

Table 21: PBS/EDTA

Reagent	[g]
Ethylenediaminetetraacetic acid tetrasodium salt dihydrate (EDTA)	0.76
1x PBS	ad 1000 ml

Table 22: 10x stock solution of MACS buffer

Reagent	[g]
Ethylenediaminetetraacetic acid tetrasodium salt dihydrate (EDTA)	0.19
Albumin, bovine fraction V powder (BSA)	1.25
1x PBS	ad 250 ml

Table 23: Anticoagulant Citrate Dextrose Solution (ACD-A)

Reagent	[g]
Citric acid monohydrate ($C_6H_8O_7 \cdot H_2O$)	0.80
Tri-sodium citrate dehydrate ($C_6H_5O_7Na_3 \cdot 2H_2O$)	2.20
Dextrose anhydrous ($C_6H_{12}O_6$)	2.20
ddH_2O	ad 100 ml

7.1.2 Density gradient centrifugation

- Dilute blood using equal volumes of PBS (pH 7.2 – 7.4)
- Overlay 5 ml of Histopaque-1077 with 5 – 7 ml of diluted blood (15 ml or 50 ml tubes)
- Centrifuge at 400x g for 30 min (w/o brake)
- Transfer 1.0 ml of plasma to a 1.5 ml reaction tube, heat-inactivate plasma at 56 °C for 15 min, and centrifuge at maximum speed for 2 min
- Transfer buffy coat cells into a new 50ml tube, add PBS/EDTA to 50ml, and centrifuge at 400x g for 10 min
- Discard supernatant, resuspend pellet in 15 ml PBS/EDTA, and pellet cells at 400x g for 10 min
- Discard supernatant, resuspend pellet in 1 ml of heat-inactivated plasma, and add PBS/EDTA to 15 ml
- Use 20 µl of cell suspension to determine total cell number using a Neubauer chamber
- Incubate on ice for 5 min
- Pellet cells in a pre-cooled centrifuge (4 – 8 °C) at 400x g for 5 min
- Resuspend cells in MACS buffer according to MACS protocol for further MACS enrichment or for cytocentrifugation onto slides.

7.1.3 Density gradient centrifugation using non-physiological conditions

- Prepare 1x Medium 199 with Earl's Salts by diluting 10x stock solution with a. dest. and adjust to pH 5.6. Dilute blood using equal volumes of 1x Medium 199 with Earl's Salts
- Immediately add 0.3 volumes of ACD-A (pH 4.9) to final pH 6.2 – pH 6.4
- Add approx. 39.2 µl of 1M NaCl per ml blood (original volume), check the osmolality, and adjust sample to 315mOsm (± 5 mOsm).
- Overlay 15 ml of Histopaque-1083 with diluted blood (50 ml tubes)
- Centrifuge at 400x g for 30 min (w/o brake)
- Transfer 1.0 ml of plasma to a 1.5 ml reaction tube, heat-inactivate plasma for at 56 °C 15 min, and centrifuge at maximum speed for 2 min

- Transfer buffy coat cells into a new 50ml tube, add PBS/EDTA to 50ml, and centrifuge at 400x g for 10 min
- Discard supernatant, resuspend pellet in 15ml of PBS/EDTA, and pellet cells at 400x g for 10 min
- Discard supernatant, resuspend pellet in 1ml of heat-inactivated plasma, and add PBS/EDTA to 15ml
- Use 20 µl of cell suspension to determine total cell number using a Neubauer chamber
- Incubate on ice for 5 min
- Pellet cells in a pre-cooled centrifuge (4 – 8 °C) at 400x g for 5 min
- Resuspend cells in MACS buffer according to MACS protocol for further MACS enrichment, or for cytocentrifugation onto slides

7.1.4 Magnetic cell separation protocol

- Resuspend density gradient enriched mononuclear cells in 80 µl of MACS buffer and 20 µl of CD71 MicroBeads per 10^7 total cells
- Incubate at 4 – 8 °C for 15 min
- Add cold MACS buffer to 10 ml and centrifuge at 400x g for 10 min using a pre-cooled centrifuge (4 – 8 °C)
- Resuspend pellet in 500µl of degassed, cold MACS buffer
- Place MACS column into MACS Separation Unit and condition column with 500 µl of degassed, cold MACS buffer
- Load cell suspension onto preconditioned MACS column
- Rinse column 3x using 500µl of degassed, cold MACS buffer
- Remove column from MACS Separation Unit and flush out cells using 1.0 ml of MACS buffer

7.2 Basic cytocentrifugation protocol

- Prepare 40µl of the respective cell suspension(s) and trypan blue (1:1 ratio) and count the cells using a Neubauer chamber
- Use MACS buffer to adjust cell suspensions to approx. 10^6 cells/ml
- Assemble slides, filter cards, and cyto buckets
- Load cyto buckets with approx. $1 \cdot 10^5$ cells per 120mm^2 and cytocentrifuge at 57x g for 5 min

- Remove access supernatants and cyto buckets
- Spin dry at 1130x g for 1 min
- Let cytospins air dry before further use

7.3 Fixation and labeling

7.3.1 Histochemistry

- Histochemical stainings used for quality checks of cytospins were performed with May-Gruenwald staining solution
- Incubate cytospin slides for 3 min using 1.5 ml of May-Gruenwald staining solution
- Add 1.5 ml of deionized water and incubate for further 8 min
- Rinse slides with deionized water and allow slides to air dry

7.3.2 Direct immunofluorescence labeling

For the following procedure incubation solutions were covered with a cover glass and incubations were performed using a humification chamber to minimize reaction volumes and to limit evaporation.

- For fixing cells add 50 µl of Reagent A (Fix&Perm Kit) onto cytospin area and incubate for 5 min
- Rinse 3x 2min in PBS

To avoid bleaching the following incubation steps were performed in the dark

- For labeling dilute FITC-antibody in AB-Diluent/20% hAB serum at 5 µg/ml, add 50 µl per cytospin area, and incubate for 30 min
- Rinse 3x 2min in PBS
- For counterstaining nuclei add 50 µl of TO-PRO-3/PBS (1:500) and incubate for 10 min
- Rinse 3x 2min in PBS
- Let air dry for a few minutes and mount the cells in mounting media (Vectashield, VectorLab)
- Store the slides in the dark until further use. When stored O/N the slides were kept at 4 – 8 °C

7.3.3 Indirectimmunofluorescencelabeling

For the following procedure incubation solutions were covered with a cover glass and incubations were performed using a humification chamber to minimize reaction volumes and to limit evaporation.

- For fixing cells add 50 µl of Reagent A onto cytospin area and incubate for 5 min
- Rinse 3x 2min in PBS

To avoid bleaching the following incubation steps were performed in the dark:

- Dilute 1° mouse-antibody in AB-Diluent/20% hAB serum at 5 µg/ml, add 50 µl per cytospin area, and incubate for 30 min
- Rinse 3x 2min in PBS
- Dilute FITC-conjugated 2° anti-mouse antibody in AB-Diluent/20% hAB serum at 5 µg/ml, add 50 µl per cytospin area, and incubate for 30 min
- Rinse 3x 2 min in PBS
- For counterstaining nuclei add 50 µl of TO-PRO-3/PBS (1:500) and incubate for 10 min
- Rinse 3x 2min in PBS
- Let air dry for a few minutes and mount the cells in mounting media (Vectashield, VectorLab)

Store the slides in the dark until further use. Storage O/N was done at 4– 8 °C

Literature

1. Sundberg K, Bang J, Smidt-Jensen S, Brocks V, Lundsteen C, Parner J, et al. Randomised study of risk of fetal loss related to early amniocentesis versus chorionic villus sampling. Lancet 1997;350(9079):697-703.
2. Hoesli IM, Walter-Gobel I, Tercanli S, Holzgreve W. Spontaneous fetal loss rates in a non-selected population. Am J Med Genet 2001;100(2):106-9.
3. Seeds JW. Diagnostic mid trimester amniocentesis: how safe? Am J Obstet Gynecol 2004;191(2):607-15.
4. Lo YM, Corbetta N, Chamberlain PF, Rai V, Sargent IL, Redman CW, et al. Presence of fetal DNA in maternal plasma and serum. Lancet 1997;350(9076):485-7.
5. Li Y, Zimmermann B, Rusterholz C, Kang A, Holzgreve W, Hahn S. Size separation of circulatory DNA in maternal plasma permits ready detection of fetal DNA polymorphisms. Clin Chem 2004;50(6):1002-11.
6. Lo YM, Tsui NB, Chiu RW, Lau TK, Leung TN, Heung MM, et al. Plasma placental RNA allelic ratio permits noninvasive prenatal chromosomal aneuploidy detection. Nat Med 2007;13(2):218-23.
7. Chim SS, Tong YK, Chiu RW, Lau TK, Leung TN, Chan LY, et al. Detection of the placental epigenetic signature of the maspin gene in maternal plasma. Proc Natl Acad Sci U S A 2005;102(41):14753-8.
8. Chan KC, Ding C, Gerovassili A, Yeung SW, Chiu RW, Leung TN, et al. Hypermethylated RASSF1A in maternal plasma: A universal fetal DNA marker that improves the reliability of noninvasive prenatal diagnosis. Clin Chem 2006;52(12):2211-8.
9. Hahn S, Ghaemmaghami F, Chitty LS. Noninvasive prenatal diagnosis: current practice and future perspectives. Curr Opin Obstet Gynecol 2008;20(2):146-51.
10. Lapaire O, Holzgreve W, Oosterwijk JC, Brinkhaus R, Bianchi DW. Georg Schmorl on trophoblasts in the maternal circulation. Placenta 2007;28(1):1-5.
11. Schmorl G. Pathologisch-anatomische Untersuchungen über Puerperal-Eklampsie. Leipzig: Verlag FCW Vogel; 1893.
12. Krabchi K, Gros-Louis F, Yan J, Bronsard M, Masse J, Forest JC, et al. Quantification of all fetal nucleated cells in maternal blood between the 18th and 22nd weeks of pregnancy using molecular cytogenetic techniques. Clin Genet 2001;60(2):145-50.
13. Krabchi K, Gadji M, Samassekou O, Gregoire MC, Forest JC, Drouin R. Quantification of fetal nucleated cells in maternal blood of pregnant women with a male trisomy 21 fetus using molecular cytogenetic techniques. Prenat Diagn 2006;26(1):28-34.
14. Bianchi DW, Flint AF, Pizzimenti MF, Knoll JH, Latt SA. Isolation of fetal DNA from nucleated erythrocytes in maternal blood. Proc Natl Acad Sci U S A 1990;87(9):3279-83.
15. Price JO, Elias S, Wachtel SS, Klinger K, Dockter M, Tharapel A, et al. Prenatal diagnosis with fetal cells isolated from maternal blood by multiparameter flow cytometry. Am J Obstet Gynecol 1991;165(6 Pt 1):1731-7.

16. Bianchi DW, Mahr A, Zickwolf GK, Houseal TW, Flint AF, Klinger KW. Detection of fetal cells with 47,XY,+21 karyotype in maternal peripheral blood. Hum Genet 1992;90(4):368-70.

17. Elias S, Simpson JL. Prenatal diagnosis of aneuploidy using fetal cells isolated from maternal blood. University of Tennessee, Memphis experience. Ann N Y Acad Sci 1994;731:80-91.

18. Guetta E, Gutstein-Abo L, Barkai G. Trophoblasts isolated from the maternal circulation: in vitro expansion and potential application in non-invasive prenatal diagnosis. J Histochem Cytochem 2005;53(3):337.

19. Mueller UW, Hawes CS, Wright AE, Petropoulos A, DeBoni E, Firgaira FA, et al. Isolation of fetal trophoblast cells from peripheral blood of pregnant women. Lancet 1990;336(8709):197-200.

20. Mavrou A, Kolialexi A, Souka A, Pilalis A, Kavalakis Y, Antsaklis P, et al. First-trimester NRBC count in maternal circulation: correlation with doppler ultrasound studies. J Histochem Cytochem 2005;53(3):315-7.

21. Troeger C, Holzgreve W, Hahn S. A comparison of different density gradients and antibodies for enrichment of fetal erythroblasts by MACS. Prenat Diagn 1999;19(6):521-6.

22. Troeger C, Zhong XY, Burgemeister R, Minderer S, Tercanli S, Holzgreve W, et al. Approximately half of the erythroblasts in maternal blood are of fetal origin. Mol Hum Reprod 1999;5(12):1162-5.

23. Mavrou A, Kouvidi E, Antsaklis A, Souka A, Kitsiou Tzeli S, Kolialexi A. Identification of nucleated red blood cells in maternal circulation: a second step in screening for fetal aneuploidies and pregnancy complications. Prenat Diagn 2007;27(2):150-3.

24. Pongsritasana T, Wongratanacheewin S, Prasertcharoensuk V, Sermswan RW. Isolation of fetal nucleated red blood cell from maternal blood using immunomagnetic beads forprenatal diagnosis. Asian Pac J Allergy Immunol 2006;24(1):65-71.

25. Christensen B, Philip J, Kolvraa S, Lykke-Hansen L, Hromadnikova I, Gohel D, et al. Fetal cells in maternal blood: a comparison of methods for cell isolation and identification. Fetal Diagn Ther 2005;20(2):106-12.

26. Kolialexi A, Vrettou C, Traeger-Synodinos J, Burgemeister R, Papantoniou N, Kanavakis E, et al. Noninvasive prenatal diagnosis of beta-thalassaemia using individual fetal erythroblasts isolated from maternal blood after enrichment. Prenat Diagn 2007;27(13):1228-32.

27. Hennerbichler S, Kroisel PM, Zierler H, Pertl B, Wintersteiger R, Dohr G, et al. Fetal nucleated red blood cells in peripheral blood of pregnant women: detection and determination of location on a slide using laser-scanning cytometry. Prenat Diagn 2003;23(9):710-5.

28. Vona G, Sabile A, Louha M, Sitruk V, Romana S, Schutze K, et al. Isolation by size of epithelial tumor cells: a new method for the immunomorphological and molecular characterization of circulating tumor cells. Am J Pathol 2000;156(1):57-63.

29. Huang R, Barber TA, Schmidt MA, Tompkins RG, Toner M, Bianchi DW, et al. A microfluidics approach for the isolation of nucleated red blood cells (NRBCs) from the peripheral blood of pregnant women. Prenat Diagn 2008;28(10):892-9.
30. Vona G, Beroud C, Benachi A, Quenette A, Bonnefont JP, Romana S, et al. Enrichment, immunomorphological, and genetic characterization of fetal cells circulating in maternal blood. Am J Pathol 2002;160(1):51-8.
31. Sitar G, Brambati B, Baldi M, Montanari L, Vincitorio M, Tului L, et al. The use of non-physiological conditions to isolate fetal cells from maternal blood. Exp Cell Res 2005;302(2):153-61.
32. Mavrou A, Kolialexi A, Antsaklis A, Korantzis A, Metaxotou C. Identification of fetal nucleated red blood cells in the maternal circulation during pregnancy using anti-hemoglobin-epsilon antibody. Fetal Diagn Ther 2003;18(5):309-13.
33. Kolvraa S, Christensen B, Lykke-Hansen L, Philip J. The fetal erythroblast is not the optimal target for non-invasive prenatal diagnosis: preliminary results. J Histochem Cytochem 2005;53(3):331-6.
34. Nagy GR, Ban Z, Sipos F, Beke A, Papp C, Papp Z. Isolation of epsilon haemoglobin-chain positive fetal cells with micromanipulation for prenatal diagnosis. Prenat Diagn 2005;25(5):398-402.
35. Christensen B, Kolvraa S, Lykke-Hansen L, Lorch T, Gohel D, Smidt-Jensen S, et al. Studies on the isolation and identification of fetal nucleated red blood cells in the circulation of pregnant women before and after chorion villus sampling. Fetal Diagn Ther 2003;18(5):376-84.
36. Christensen B, Philip J, Lykke-Hansen L, Kolvraa S. Sensitivity and specificity of the identification of fetal cells in maternal blood by combined staining with antibodies against beta, gamma- and epsilon-globin chains. Fetal Diagn Ther 2003;18(6):479-84.
37. Mergenthaler S, Babochkina T, Kiefer V, Lapaire O, Holzgreve W, Hahn S. FISH analysis of all fetal nucleated cells in maternal whole blood: improved specificity by the use of two Y-chromosome probes. J Histochem Cytochem 2005;53(3):319-22.
38. Krabchi K, Gadji M, Forest JC, Drouin R. Quantification of all fetal nucleated cells in maternal blood in different cases of aneuploidies. Clin Genet 2006;69(2):145-54.
39. Bianchi DW, Zickwolf GK, Weil GJ, Sylvester S, DeMaria MA. Male fetal progenitor cells persist in maternal blood for as long as 27 years postpartum. Proc Natl Acad Sci U S A 1996;93(2):705-8.
40. Kolialexi A, Tsangaris GT, Antsaklis A, Mavrou A. Fetal cells in maternal plasma are found in a late state of apoptosis. Prenat Diagn 2004;24(9):719-21.
41. Babochkina T, Mergenthaler S, De Napoli G, Hristoskova S, Tercanli S, Holzgreve W, et al. Numerous erythroblasts in maternal blood are impervious to fluorescent in situ hybridizationanalysis, a feature related to a dense compact nucleus with apoptotic character. Haematologica 2005;90(6):740-5.

42. Kondo T, Sekizawa A, Saito H, Jimbo M, Sugito Y, Okai T. Fate of fetal nucleated erythrocytes circulating in maternal blood: apoptosis is induced by maternal oxygen concentration. Clin Chem 2002;48(9):1618-20.
43. Kumar SS, Ghosh A, Devasagayam TP, Chauhan PS. Effect of vanillin on methylene blue plus light-induced single-strand breaks in plasmid pBR322 DNA. Mutat Res 2000;469(2):207-14.
44. Epe B, Hegler J, Wild D. Singlet oxygen as an ultimately reactive species in Salmonella typhimurium DNA damage induced by methylene blue/visible light. Carcinogenesis 1989;10(11):2019-24.
45. Boiteux S, Gajewski E, Laval J, Dizdaroglu M. Substrate specificity of the Escherichia coli Fpg protein (formamidopyrimidine-DNA glycosylase): excision of purine lesions in DNA produced by ionizing radiation or photosensitization. Biochemistry 1992;31(1):106-10.
46. Choolani M, O'Donoghue K, Talbert D, Kumar S, Roberts I, Letsky E, et al. Characterization of first trimester fetal erythroblasts for non-invasive prenatal diagnosis. Mol Hum Reprod 2003;9(4):227-35.
47. Cha DH, Khosrotehrani K, Bianchi DW, Johnson KL. The utility of an erythroblast scoring system and gender-independent short tandem repeat (STR) analysis for the detection of aneuploid fetal cells in maternal blood. Prenat Diagn 2005;25(7):586-91.
48. Choe J, Hwang D, Kim KC, Choi YM. Fetal gender determination and BclI polymorphism using nucleated erythrocytes in maternal blood. J Histochem Cytochem 2005;53(3):323-7.
49. Mesker WE, Ouwerkerk-van Velzen MC, Oosterwijk JC, Bernini LF, Golbus MS, Kanhai HH, et al. Two-colour immunocytochemical staining of gamma (gamma) and epsilon (epsilon) type haemoglobin in fetal red cells. Prenat Diagn 1998;18(11):1131-7.
50. Tjoa ML, Delli-Bovi L, Johnson KL, Bianchi DW. Antibodies to trophoblast antigens HLA-G, placenta growth factor, and neuroD2 do not improve detection of circulating trophoblast cells in maternal blood. Fetal Diagn Ther 2007;22(2):85-9.
51. Cioni R, Bussani C, Scarselli B, Bucciantini S, Marchionni M, Scarselli G. Comparison of two techniques for transcervical cell sampling performed in the same study population. Prenat Diagn 2005;25(3):198-202.
52. Katz-Jaffe MG, Mantzaris D, Cram DS. DNA identification of fetal cells isolated from cervical mucus: potential for early non-invasive prenatal diagnosis. Bjog 2005;112(5):595-600.
53. Cioni R, Bussani C, Scarselli B, Bucciantini S, Barciulli F, Scarselli G. Fetal cells in cervical mucus in the first trimester of pregnancy. Prenat Diagn 2003;23(2):168-71.
54. Cioni R, Bussani C, Scarselli B, Barciulli F, Bucciantini S, Simi P, et al. Detection of fetal cells in intrauterine lavage samples collected in the first trimester of pregnancy. Prenat Diagn 2002;22(1):52-5.
55. Bussani C, Cioni R, Mattei A, Fambrini M, Marchionni M, Scarselli G. Prenatal diagnosis of common aneuploidies in transcervical samples using quantitative fluorescent-PCR analysis. Mol Diagn Ther 2007;11(2):117-21.

56. Bulmer JN, Cioni R, Bussani C, Cirigliano V, Sole F, Costa C, et al. HLA-G positive trophoblastic cells in transcervical samples and their isolation and analysis by laser microdissection and Q-PCR. Prenat Diagn 2003;23(1):34-9.
57. Adinolfi M, Sherlock J. Fetal cells in transcervical samples at an early stage of gestation. J Hum Genet 2001;46(3):99-104.
58. Adinolfi M, Davies A, Sharif S, Soothill P, Rodeck C. Detection of trisomy 18 and Y-derived sequences in fetal nucleated cells obtained by transcervical flushing. Lancet 1993;342(8868):403-4.
59. Tanke HJ, Oosterwijk JC, Mesker WE, Ouwerkerk van-Velzen MC, Knepfle CF, Wiesmeyer CC, et al. Detection of 'rare event' fetal erythroblasts in maternal blood using automated microscopy. Early Hum Dev 1996;47 Suppl:S89-93.
60. Oosterwijk JC, Knepfle CF, Mesker WE, Vrolijk H, Sloos WC, Pattenier H, et al. Strategies for rare-event detection: an approach for automated fetal cell detection in maternal blood. Am J Hum Genet 1998;63(6):1783-92.
61. Mehes G, Lorch T, Ambros PF. Quantitative analysis of disseminated tumor cells in the bone marrow by automated fluorescence image analysis. Cytometry 2000;42(6):357-62.
62. Kilpatrick MW, Tafas T, Evans MI, Jackson LG, Antsaklis A, Brambati B, et al. Automated detection of rare fetal cells in maternal blood: eliminating the false-positive XY signals in XX pregnancies. Am J Obstet Gynecol 2004;190(6):1571-8; discussion 1578-81.
63. Hartmann M, Blaschitz A, Hammer A, Haidacher S, Mahnert W, Walcher W, et al. Immunohistochemical examination of trophoblast populations in human first trimester and term placentae and of first trimester spiral arteries with the monoclonal antibody GZ 112. Placenta 1997;18(7):481-9.
64. Goding JW. Production of monoclonal antibodies 2 ed. London: Academic Press; 1983.
65. Hiden U, Maier A, Bilban M, Ghaffari-Tabrizi N, Wadsack C, Lang I, et al. Insulin control of placental gene expression shifts from mother to foetus over the course of pregnancy. Diabetologia 2006;49(1):123-31.
66. Butler JM, Reeder DJ. Short Tandem Repeat DNA Internet DataBase. In: National Institute of Standards and Technology; 1997.
67. Schmidt U, Lutz-Bonengel S, Weisser HJ, Sanger T, Pollak S, Schon U, et al. Low-volume amplification on chemically structured chips using the PowerPlex16 DNA amplification kit. Int J Legal Med 2006;120(1):42-8.
68. Hagen-Mann K, Zacher T, Khanaga O, Baukloh V, Mann W, Schön U. Molekularbiologische Analyse von Einzelzellen. medizinischegenetik 2005;17:53-59.
69. Dietmaier W, Hartmann A, Wallinger S, Heinmoller E, Kerner T, Endl E, et al. Multiple mutation analyses in single tumor cells with improved whole genome amplification. Am J Pathol 1999;154(1):83-95.
70. Chen HP, Wang TR, Xu JP, Xu XY, Dangol SD, He GF. Fetal origin of single nucleated erythroblasts and free DNA in the peripheral blood of pregnant women. Int J Gynaecol Obstet 2004;85(1):1-5.

71. Yang YH, Yang ES, Kwon JY, Kim IK, Park YW. Prenatal diagnosis of trisomy 21 with fetal cells in maternal blood using comparative genomic hybridization. Fetal Diagn Ther 2006;21(1):125-33.

72. Garvin AM, Holzgreve W, Hahn S. Highly accurate analysis of heterozygous loci bysingle cell PCR. Nucleic Acids Res 1998;26(15):3468-72.

73. Hahn S, Zhong XY, Troeger C, Burgemeister R, Gloning K, Holzgreve W. Current applications of singlecell PCR. Cell Mol Life Sci 2000;57(1):96-105.